Optimizing shifted stabilizers with asymmetric input saturation

Philipp Braun, Giulia Giordano, Christopher M. Kellett, Iman Shames, Luca Zaccarian

Optimizing shifted stabilizers with asymmetric input saturation

P. Braun, G. Giordano, C. M. Kellett, I. Shames, and L. Zaccarian

***Abstract*— We develop a controller design for linear systems subject to asymmetric actuator saturation that maximizes the estimate of the region of attraction of the corresponding closed-loop system. Stabilization is achieved by stabilizing shifted equilibria selected via the solution of an optimization problem enjoying desirable asymptotic properties. To enable the computational time required by these optimizers, we impose sampled-data updates of these equilibria and cast our description within a hybrid dynamical systems formulation. We provide two feedback solutions using exact and inexact optimization algorithms, thus establishing interesting interplays between continuous-time dynamics and iterative discrete-time parametric optimization schemes. Enlarged estimates of the region of attraction and the real-time applicability of the control law are illustrated on numerical examples.**

I. Introduction

Linear matrix inequalities (LMIs) and semidefinite programming [8] have become a standard tool to estimate regions of attraction in terms of sublevel sets of Lyapunov functions and to design controllers for linear systems subject to input saturation constraints [19], [31]. Software interfaces such as CVX [16], SOSTOOLS [28] or YALMIP [25], for example, provide a straightforward way to set up optimization problems subject to LMIs and to efficiently compute solutions from which control Lyapunov functions, controller gains and estimates of the region of attraction can be recovered.

While most approaches focus on symmetric saturation bounds, asymmetric limits often arise in practice [19], [20]. Thus, when applied to systems with asymmetric input constraints, results focusing on symmetric bounds are in general suboptimal and conservative.

LMI-based controller designs for linear systems specifically taking asymmetric saturations into account are rarely found in the literature. The monograph [24] dedicates one chapter to asymmetric saturations and the chapter relies on the results derived in the paper [22]. Some relevant examples using this technique are also discussed in [24, Chapter 9.4].

P. Braun and L. Zaccarian are supported in part by the Agence Nationale de la Recherche (ANR) via grant "Hybrid And Networked Dynamical sYstems" (HANDY), number ANR-18-CE40-0010.

P. Braun, C. M. Kellett and I. Shames are with CIICADA Lab, School of Engineering, Australian National University, Canberra, Australia. {philipp.braun,chris.kellett,iman.shames}@anu.edu.au

G. Giordano is with the Department of Industrial Engineering, University of Trento, Trento, Italy. giulia.giordano@unitn.it

L. Zaccarian is with the LAAS-CNRS, Université de Toulouse, Toulouse, France and with the Department of Industrial Engineering, University of Trento, Trento, Italy. luca.zaccarian@laas.fr

Existing approaches focusing on asymmetric actuator constraints include the use of nonsymmetric Lyapunov certificates for symmetric stabilizers [4], [20]. Piecewise quadratic Lyapunov functions with symmetric stabilizing saturated linear feedbacks are used in [23] and [17], in the continuous-time and discrete-time cases, respectively. In [5, Ch. 8] a shifted equilibrium is stabilized, which comes at the cost that convergence of solutions to the origin is no longer guaranteed. In [32], a switching dynamical controller is designed to exploit the available range of the control action on both sides of the saturation levels. A common feature of the above-mentioned results is that a single Lyapunov function is used to characterize solutions in the domain of interest.

An alternative approach may comprise gradually shifting a reference x_e to the origin, a point to be stabilized by a linear feedback controller, following a gain scheduling approach [30].

Alternative solutions taking constraints directly into account in the controller design process are model predictive control (see [18] or [29] for general references) and reference governors, for example. Explicit model predictive control can handle linear systems with symmetric or asymmetric input saturation levels in an explicit controller design [3], [15]. However, explicit model predictive control derives a control law based on discrete-time systems in general, whereas here we address the problem in the continuous-time setting.

In this paper, we follow a scheduling paradigm where a Lyapunov certificate is applied in shifted coordinates, whose shifting parameter is adapted in a sample-and-hold fashion. Our approach is inspired by the work in [7]; it is motivated by the work in [26], and it extends the subsequent publication [10]. The paper [7] discusses controllability of constrained linear systems and the maximal size of regions of attraction of appropriately selected feedback laws. The ideas in [7] are used in [26] to propose an asymmetric stabilizer for systems of the form

$$\dot{x} = Ax + B\sigma, \quad \sigma \in [-u^-, u^+], \quad u^-, u^+ \in \mathbb{R}^m_{>0}, \qquad (1)$$

(where $m \in \mathbb{N}$) based on convex scaling of a shifted stabilizer. Through the shifted stabilizer, significantly larger guarantees are obtained in terms of the estimate of regions of attraction (abbreviated as ERA in the following). However, this comes at the cost of reduced local performance. Our recent paper [10] overcomes the issues with local performance and extends the ideas in [26] while further increasing the size of the estimate of the region of attraction. The results in [10] are restricted to systems with one dimensional input $m = 1$. In this paper, we

discuss a nontrivial extension for the general m-dimensional setting. Moreover, we remove the assumption that the matrix A in (1) be nonsingular. Removing this assumption enables results extending the estimate of the region of attraction to infinity in some suitable directions. While we focus on asymmetric saturations, we also obtain improved results for symmetric saturations as a special case. Our work, starting from a suitable symmetric stabilizer of the origin, first exploits linearity to obtain a stabilizing feedback law for any shifted equilibrium of the form

$$x_e \in \{x \in \mathbb{R}^n : \ Ax + B\sigma = 0, \ \sigma \in \mathbb{R}^m\}. \tag{2}$$

Then, we design a controller that gradually shifts the reference point x_e to the origin. Through this process, the ERA of the origin of the overall closed-loop system is characterized as the union of the ERAs associated with each of the considered shifted equilibria.

In [10], for the single-input case, we could explicitly solve an optimization problem, which allowed us to implement a continuous update of the shifted equilibrium x_e. For the multi-input case addressed here, such a solution is not viable. Therefore we embed the continuous-time feedback in a hybrid systems framework [14], where x_e is updated at discrete time steps. In this context, we analyze the interplay between the continuous-time evolution of (1) and state-dependent discrete-time updates of x_e ruled by iterative parametric optimization schemes. Consequently an interesting interaction of feedback control and optimization emerges.

The approach discussed here is closely related to reference governors, or more precisely Lyapunov and invariance based explicit reference governors. See [12], [13] and [27] for origins and overviews on these approaches, for example. Explicit reference governors, as described in [27], augment pre-defined control laws designed for unconstrained dynamics to additionally take input and state constraints into account. Then, similar to the approach discussed here, instead of stabilizing the target set directly, a reference point is stabilized for which constraints described through inequalities can be shown to be satisfied. The reference point is updated through a navigation field and constraint satisfaction is guaranteed through a function capturing a dynamic safety margin. As opposed to explicit reference governors, in this paper, an explicit expression of the viable set in terms of inequality constraints is not known. Thus, we are not using navigation fields and safety margins here, but update the reference point by using an appropriately selected optimization problem and by leveraging forward invariance, convexity and Lyapunov arguments.

The paper is structured as follows. In Section II the problem formulation is defined and a feedback law based on the shifted equilibrium is introduced. In Section III we introduce the optimization problem behind the selection of the shifted equilibrium x_e and establish its properties. Then, Section IV discusses a feedback law requiring the exact solution of this optimization problem. Section V extends the results of Section IV to a more general setting with inexact optimizers and iterative parametric optimization schemes. The results of the paper are illustrated through numerical examples in Section VI before the paper concludes with final remarks in Section VII.

Notation. For $u^-, u^+ \in \mathbb{R}^m_{\geq 0}$, $m \in \mathbb{N}$, $\operatorname{sat}_{[u^-,u^+]}(u) = \max\{\min\{u^+, u\}, -u^-\}$ defines the saturation, where the maximum/minimum are to be understood componentwise. The deadzone is defined as $\operatorname{dz}_{[u^-,u^+]}(u) = u - \operatorname{sat}_{[u^-,u^+]}(u)$. For $Z \in \mathbb{R}^{n\times n}$, $\operatorname{He}(Z) = Z + Z^\top$. For $Z \in \mathbb{R}^{n\times m}$ and $z \in \mathbb{R}^n$, $Z_{[k]}$ and z_k denote the k-th row and the k-th entry, respectively. A vector $v \in \mathbb{R}^n$ satisfies $v \leq \min\{u^-, u^+\}$ if $v_k \leq \min\{u_k^-, u_k^+\}$ for all $k \in \{1, \dots, n\}$. A positive definite matrix $P \in \mathbb{R}^{n\times n}$ can be uniquely decomposed as $P = P^{\frac{1}{2}}P^{\frac{1}{2}}$ where $P^{\frac{1}{2}} \in \mathbb{R}^{n\times n}$ is positive definite. In $\mathbb{R}^n$, we use the norms $|x| = \sqrt{x^\top x}$, $|x|_P = \sqrt{x^\top P x}$ and $P \in \mathbb{R}^{n\times n}$ positive definite, while $\lambda_{\min}(P)$, $\lambda_{\max}(P)$ denote the smallest and largest eigenvalues of the symmetric matrix P. For $A \in \mathbb{R}^{n\times m}$ the spectral norm is denoted by $\|A\|_2 = \sqrt{\lambda_{\max}(A^\top A)}$. Moreover, $I \in \mathbb{R}^{n\times n}$ denotes the identity matrix, $\mathbb{1}$ satisfies $\mathbb{1}_k = 1$, $k \in \{1, \dots, n\}$, and $\operatorname{int}(\mathcal{A})$, $\overline{\mathcal{A}}$ denote the interior and the closure of a set $\mathcal{A} \subset \mathbb{R}^n$, respectively. Given two vectors $x_1 \in \mathbb{R}^n$, $x_2 \in \mathbb{R}^m$, for the augmented vector the following notation is used: $(x_1, x_2) = [x_1^\top \ x_2^\top]^\top \in \mathbb{R}^{n+m}$.

II. Symmetric and shifted stabilizers

We consider linear saturated continuous-time systems

$$\dot{x} = Ax + B \operatorname{sat}_{[u^-,u^+]}(u) \tag{3}$$

with state $x \in \mathbb{R}^n$, input $u \in \mathbb{R}^m$, $A \in \mathbb{R}^{n\times n}$, $0 \neq B \in \mathbb{R}^{n\times m}$ and saturation limits $u^-, u^+ \in \mathbb{R}^m_{>0}$. We define the average saturation range and the average saturation center as

$$\bar{u} := \tfrac{1}{2}(u^+ + u^-), \quad u_\circ := \tfrac{1}{2}(u^+ - u^-), \tag{4}$$

respectively. For simplicity, we assume that the components of the average saturation range $\bar{u}_k$ satisfy $\bar{u}_k = 1$ for all $k \in \{1, \dots, m\}$; this is not restrictive and can always be assumed without loss of generality for $u^-, u^+ \in \mathbb{R}^m_{>0}$ by scaling the columns of B. Additionally, to define a stabilizing control law, we need to assume that the pair (A, B) be stabilizable.

Assumption 1: It holds that $\bar{u} = \mathbb{1} \in \mathbb{R}^m$ and the pair (A, B) is stabilizable. ◇

The subspace of pairs of induced equilibria

$$\Gamma := \{(x_e, u_e) \in \mathbb{R}^n \times \mathbb{R}^m : \ Ax_e + Bu_e = 0\}. \tag{5a}$$

can be characterized through the kernel of the matrix $[A \ B]$. In particular, there exist $A^\perp \in \mathbb{R}^{n\times p}$ and $B^\perp \in \mathbb{R}^{m\times p}$ such that

$$\Gamma = \{(A^\perp \rho, B^\perp \rho) \in \mathbb{R}^n \times \mathbb{R}^m : \rho \in \mathbb{R}^p\} \tag{5b}$$

and the columns of $\begin{bmatrix} A^\perp \\ B^\perp \end{bmatrix}$ are a basis of the p-dimensional subspace of the kernel of $[A \ B]$.

Using the notation of the kernel, we may define linear mappings from $\mathbb{R}^m$ to the set of induced equilibria as $x_e(\cdot) : \mathbb{R}^p \to \mathbb{R}^n$, $u_e(\cdot) : \mathbb{R}^p \to \mathbb{R}^m$ with $x_e(\rho) = A^\perp \rho$, $u_e(\rho) = B^\perp \rho$, depending on the shifting parameter ρ.

In the definition of Γ, the saturation levels are not present. System (3) with $u \in [-u^-, u^+]$ (to be understood componentwise) can only be stabilized at $x_e(\rho)$ if a corresponding input satisfies $u_e(\rho) \in [-u^-, u^+]$. The corresponding domain can be defined with respect to the shifting parameter ρ as

$$\Phi = \{\rho \in \mathbb{R}^p : \ -u^- \leq B^\perp \rho \leq u^+\}. \tag{6}$$

In a neighborhood of the origin, we will use a feedback law

$$u = Kx + L\,\mathrm{dz}_{[u^-,u^+]}(u), \tag{7}$$

with $K \in \mathbb{R}^{m\times n}$, $L \in \mathbb{R}^{m\times m}$, to asymptotically stabilize the origin. Combining (3) and (7), the closed-loop dynamics are given by

$$\begin{aligned} \dot{x} &= (A+BK)x - (B-BL)\,\mathrm{dz}_{[u^-,u^+]}(u) \\ u &= Kx + L\,\mathrm{dz}_{[u^-,u^+]}(u). \end{aligned} \tag{8}$$

To characterize regions of attraction of asymptotically stable (induced) equilibria $x_e(\rho)$, we consider sublevel sets of quadratic functions

$$\mathcal{E}_\rho(P) = \{x \in \mathbb{R}^n : \ |x - x_e(\rho)|_P \leq \beta(\rho)\}, \tag{9}$$

where $\rho \in \Phi$, $P \in \mathbb{R}^{n\times n}$ and the function $\beta : \mathbb{R}^p \to \mathbb{R}$ is defined as

$$\begin{aligned} \beta(\rho) &= \min\{\min\{u^- + B^\perp\rho, u^+ - B^\perp\rho\}\} \\ &= \min\{\min\{u^- + u_e(\rho), u^+ - u_e(\rho)\}\}. \end{aligned} \tag{10}$$

Here, $\min : \mathbb{R}^p \times \mathbb{R}^p \to \mathbb{R}^p$ defines the componentwise minimum of two vectors, i.e.,

$$\min_i\{a,b\} = \min\{a_i, b_i\}, \quad i \in \{1,\dots,p\},$$

while $\min : \mathbb{R}^p \to \mathbb{R}$ defines the minimum of a vector, i.e., $\min\{a\} = \min_{i\in\{1,\dots,p\}} a_i$. Note that under Assumption 1, and in particular due to the property $\overline{u} = \mathbb{1}$, it holds that $\beta : \Phi \to [0,1]$, i.e., $\beta(\cdot)$ restricted to the set Φ, implicitly describing the set of induced equilibria of interest, is lower and upper bounded by 0 and 1, respectively.

Instead of stabilizing the origin, we can stabilize an induced equilibrium $x_e(\rho)$ by considering the shifted coordinates $\widetilde{x} := x - x_e(\rho)$, $\widetilde{u} := u - u_e(\rho)$. For the shifted coordinates it holds that

$$\begin{aligned} \dot{\widetilde{x}} &= \dot{x} = Ax + B\,\mathrm{sat}_{[u^-,u^+]}(u) \\ &= A\widetilde{x} + Ax_e(\rho) + B(u_e(\rho) + \mathrm{sat}_{[u^- + u_e(\rho), u^+ - u_e(\rho)]}(\widetilde{u})) \\ &= A\widetilde{x} + B\,\mathrm{sat}_{[u^- + u_e(\rho), u^+ - u_e(\rho)]}(\widetilde{u}), \end{aligned} \tag{11}$$

where the plant input is selected as

$$u = k(x,\rho) := u_e(\rho) + \widetilde{u}, \tag{12}$$

$$\widetilde{u} = K(x - x_e(\rho)) + L\,\mathrm{dz}_{[u^- + u_e(\rho), u^+ - u_e(\rho)]}(\widetilde{u}), \tag{13}$$

and $\widetilde{u}$ is implicitly defined by the algebraic constraint (13).

With these definitions the following result summarizes Proposition 1 and Corollaries 1 and 2 in [10].

Proposition 1: Given the plant (3), let $\bar{u} = \mathbb{1} \in \mathbb{R}^m$ and let $\alpha \in \mathbb{R}_{\geq 0}$. Moreover, let $Q \in \mathbb{R}^{n\times n}$, $W, Y \in \mathbb{R}^{m\times n}$, $U, X \in \mathbb{R}^{m\times m}$ be a solution of the optimization problem

$$\begin{aligned} \max_{Q,W,Y,U,X} \quad & \log\det(Q) \\ \text{subject to} \quad & U > 0 \ \text{ diagonal}, \quad Q = Q^\top > 0 \\ & \mathrm{He}\begin{bmatrix} AQ + BW + \alpha Q & -BU + BX \\ W + Y & X - U \end{bmatrix} < 0 \\ & \begin{bmatrix} 1 & Y_{[k]} \\ Y_{[k]}^\top & Q \end{bmatrix} \geq 0, \quad k = 1,\dots,m. \end{aligned} \tag{14}$$

Then, for

$$K = WQ^{-1}, \quad L = XU^{-1}, \quad P = Q^{-1} \tag{15}$$

the nonlinear algebraic loop in (13) is well posed (i.e., its solution is unique and Lipschitz) and for each $\rho \in \mathrm{int}(\Phi)$ the Lyapunov function

$$V_\rho(x) := |x - x_e(\rho)|_P^2 = (x - x_e(\rho))^\top P (x - x_e(\rho))$$

exponentially decreases with rate larger than 2α within the set $\mathcal{E}_\rho(P)$ in (9), i.e., $\dot{V}_\rho(x(t)) \leq -2\alpha V_\rho(x(t))$ for all $x \in \mathcal{E}_\rho(P)$. Consequently, the induced equilibrium $x_e(\rho)$ of the plant (8) is locally exponentially stable, with region of attraction containing $\mathcal{E}_\rho(P)$. ⌟

Remark 1: For $L \neq 0$, the feedback law (12) is only defined implicitly through the algebraic condition (13). Nevertheless, as discussed in Proposition 1, it is well-defined. If $u \in \mathbb{R}$ (i.e., $m = 1$), $\widetilde{u}$ can be defined explicitly (see [26, Lemma 3] or [10, Remark 1], for example). Efficient solutions of the algebraic loop in higher dimensions $m > 1$ are discussed in [6]. The algebraic loop can be avoided by setting $X = 0$, and thus $L = 0$, in Proposition 1. In this case the feedback law k reduces to $k(x,\rho) = u_e(\rho) + K(x - x_e(\rho))$. While this restriction is more conservative with respect to the region of attraction, the control law is sufficient to highlight the advantages of the controller design discussed in this paper. ∘

To simplify the notation of the closed-loop system (11) with input (12), let us introduce

$$\begin{aligned} \dot{x} =& f(x, k(x,\rho)) := Ax + B\,\mathrm{sat}_{[u^-,u^+]}(k(x,\rho)) \\ =& A(x - x_e(\rho)) + B\,\mathrm{sat}_{[u^- + u_e(\rho), u^+ - u_e(\rho)]}(\widetilde{u})) \end{aligned} \tag{16}$$

where k is defined in (12) and the second equality holds because $\rho \in \mathrm{int}(\Phi)$.

Remark 2: The decrease condition of the Lyapunov function V_ρ established in Proposition 1 is equivalent to

$$(x - x_e(\rho))^\top P f(x, k(x,\rho)) \leq -\alpha V_\rho(x), \tag{17}$$

for all $x \in \mathcal{E}_\rho(P)$. ∘

III. Optimization-based shifted stabilizer

Even though the result of Proposition 1 applies to arbitrary induced equilibria, we are interested in the stabilization of the origin in this paper. Thus, to stabilize the origin, we need to make use of the degree of freedom ρ in the feedback law k defined in (12). In particular, to enlarge the ERA of our stabilizing feedback, we will make use of the parametric feedback law (12) and consider the sets

$$\mathcal{R} := \bigcup_{\rho\in\mathrm{int}(\Phi)} \mathcal{E}_\rho(P), \qquad \overline{\mathcal{R}} = \bigcup_{\rho\in\Phi} \mathcal{E}_\rho(P), \tag{18}$$

comprising the union of all the ERAs established by Proposition 1 for each $x_e(\rho)$, $\rho \in \mathrm{int}(\Phi)$ and its closure. Note that $\mathcal{R}$ is neither closed nor open as a subset of $\mathbb{R}^n$, but it holds that $\mathrm{int}(\mathcal{R}) = \mathrm{int}(\overline{\mathcal{R}})$.

To select ρ in our feedback law (12)-(13) and (16), we first focus on the optimization problem

$$\begin{aligned} \rho^\star(x) := \underset{\delta \in \Phi}{\operatorname{argmin}} \ & |\delta|^2 \\ \text{subject to} \ & |x - x_e(\delta)|_P \leq \beta(\delta) \end{aligned} \tag{19}$$

for all $x \in \overline{\mathcal{R}}$. In Lemma 1 in Section III-A, it will be shown that for all $x \in \overline{\mathcal{R}}$ the minimizer of (19) exists and is unique, and thus $\rho^\star(\cdot)$ is indeed well defined. Through $\rho^\star(x)$, the optimization problem indirectly defines an induced equilibrium $x_e(\rho^\star(x))$ such that x is in the ERA provided by Proposition 1, while the distance of $\rho^\star$ to the origin is minimized.

A. Properties of the optimization problem (19)

In this section we analyze the properties of (19), as a function of $x \in \overline{\mathcal{R}}$ defined in (18). A related result has been derived in [10, Lemma 1] for one-dimensional ρ.

Lemma 1: Under Assumption 1, consider the optimization problem (19) where β and $\mathcal{R}$ are defined in (10) and (18), respectively, and matrix P is defined through Proposition 1. Then the following properties are satisfied:

1) for each $x \in \overline{\mathcal{R}}$, (19) is feasible, and the feasible set is closed and convex. Moreover, for $x \in \mathrm{int}(\mathcal{R})$ the interior of the feasible set is nonempty;
2) the set-valued map $F : \overline{\mathcal{R}} \rightrightarrows \Phi$,
$$F(x) = \{\rho \in \Phi : \ |x - x_e(\rho)|_P \leq \beta(\rho)\},$$
defining the feasible set of (19), is continuous;
3) $\rho^\star(x) = 0$ for all $x \in \overline{\mathcal{R}}$ such that $|x|_P \leq \beta(0)$;
4) $|x - x_e(\rho^\star(x))|_P = \beta(\rho^\star(x))$ for all $x \in \overline{\mathcal{R}}$ such that $|x|_P > \beta(0)$;
5) $\rho^\star(x) \in \Phi$ is unique for all $x \in \overline{\mathcal{R}}$;
6) $\rho^\star(\cdot) : \overline{\mathcal{R}} \to \Phi$ is continuous; and
7) $\rho^\star(x) \in \mathrm{int}(\Phi)$ for all $x \in \mathrm{int}(\mathcal{R})$. ⌟

Proof: Item 1. Feasibility follows immediately from the definitions of β and the set $\overline{\mathcal{R}}$. Closedness of the feasible set follows from continuity of $|x - A^\perp(\cdot)|_P$ and $\beta(\cdot)$ and the nonstrict inequality in (19). Convexity of the feasible set follows from the fact that the function $|x - A^\perp(\cdot)|_P - \beta(\cdot)$ is convex. In particular, for $x \in \overline{\mathcal{R}}$ and $\rho_1, \rho_2 \in \Phi$ such that $|x - A^\perp \rho_1|_P \leq \beta(\rho_1)$, $|x - A^\perp \rho_2|_P \leq \beta(\rho_2)$, for all $\lambda \in [0, 1]$, it holds that

$$\begin{aligned} |x - x_e(\lambda\rho_1 + (1-\lambda)\rho_2)|_P &= |x - A^\perp(\lambda\rho_1 + (1-\lambda)\rho_2)|_P \\ &\leq \lambda\beta(\rho_1) + (1-\lambda)\beta(\rho_2) \leq \beta(\lambda\rho_1 + (1-\lambda)\rho_2). \end{aligned} \tag{20}$$

Finally, for $x \in \mathrm{int}(\mathcal{R})$ fixed, there exists $\bar{\rho} \in \mathrm{int}(\Phi)$ such that $|x - A^\perp \bar{\rho}|_P < \beta(\bar{\rho})$. Otherwise, x needs to be on the boundary of $\mathcal{R}$, which contradicts the assumptions. Since $|x - A^\perp(\cdot)|_P$ and $\beta(\cdot)$ are continuous and since $\bar{\rho} \in \mathrm{int}(\Phi)$, there exists $\varepsilon > 0$ such that $|x - A^\perp \rho|_P \leq \beta(\rho)$ and $\rho \in \mathrm{int}(\Phi)$ for all ρ such that $|\bar{\rho} - \rho| \leq \varepsilon$, which shows that the interior of the feasible set is nonempty.

Item 2. Continuity of F follows from the properties established in item 1 together with [11, Example 3B.4] (or [11, Theorem 3B.3]). In particular, (20) shows that $g(x, \cdot) = |x - A^\perp(\cdot)|_P - \beta(\cdot)$ is convex on the domain of interest.

Item 3. This property follows immediately from $|x|_P \leq \beta(0)$ and the objective function in (19).

Item 4. To obtain a contradiction, assume that $|x - x_e(\rho^\star)|_P < \beta(\rho^\star)$. Since $|x|_P \geq \beta(0)$ it follows that $\rho^\star \neq 0$. Since $x_e(\cdot)$ and $|\cdot|^2$ are continuous, there exists $\rho^\# \in \Phi$ with $|\rho^\#|^2 < |\rho^\star|^2$ and $|x - x_e(\rho^\#)|_P < \beta(\rho^\#)$, which contradicts the optimality of $\rho^\star$ and thus completes the proof.

Item 5. Since the feasible set is closed, convex and compact (see item 1) and the objective function is continuous, the minimum $|\rho^\star(x)|^2$ in (19) is attained through $\rho^\star(x) \in F(x) \subset \Phi$. Moreover, since the objective function is strictly convex, $\rho^\star(x) \in \Phi$ is unique.

Item 6. Since $F(\cdot)$ is continuous and due to the selection of the objective function, $\rho^\star(\cdot)$ is continuous (see [2, Ch. 1, Sec. 7, Thm. 1] and [1, Ch. 6.5.1]).

Item 7. The statement follows from the fact that $F(x)$ is convex with nonempty interior for all $x \in \mathrm{int}(\mathcal{R})$, convexity of the set Φ containing the origin in its interior and the objective function minimizing the distance to the origin. ■

Remark 3: Note that Lemma 1, Item 6, establishes continuity on a closed set $\overline{\mathcal{R}} \subset \mathbb{R}^n$. Here, $\rho^\star(\cdot)$ should be understood as a mapping from the metric space $\overline{\mathcal{R}}$ to the metric space Φ in terms of the definition of continuity to ensure that continuity on the boundary of $\overline{\mathcal{R}}$ be well defined. ◦

Remark 4: In the sequel, we study asymptotic stability of the origin by restricting the attention to the set $x \in \mathrm{int}(\mathcal{R})$. This restriction ensures that $\rho^\star(x) \in \mathrm{int}(\Phi)$ according to Lemma 1, item 7. This is important, because for any $\bar{\rho} \in \Phi \setminus \mathrm{int}(\Phi)$ we have $\beta(\bar{\rho}) = 0$ and Proposition 1 provides the trivial ERA $\mathcal{E}_{\bar{\rho}}(P) = \{x_e(\bar{\rho})\}$, which is useless and thus should be avoided. Instead, for $x \in \mathrm{int}(\mathcal{R})$, Proposition 1 characterizes an ellipsoid $\mathcal{E}_{\rho^\star(x)}(P)$ with nonzero volume. ◦

B. Sampled-data update of the shifting parameter

Under the assumption that an explicit expression of the (unique) solution $\rho^\star : \overline{\mathcal{R}} \to \Phi$ of (19) is available, controller (12) is implementable and stability of the origin of the closed loop $\dot{x} = f(x, k(x, \rho^\star(x)))$ can be investigated. However, in this paper we assume that such an explicit solution is not available and the time to solve (19) is not negligible. Thus, we implement a piecewise constant selection of ρ in (12) and (16), updated in a sampled-data fashion when the solution $\rho^\star(\chi)$ of (19) for a sample-and-hold version χ of the state x becomes available. (The definition of the state χ is made precise later in (34).)

Remark 5: If ρ is one dimensional, i.e., $p = 1$, an explicit solution of (19) can be derived [10]. In this case a continuous update of ρ is not restrictive in terms of the implementation of the control law. In this paper, we explicitly focus on the multi-input case where an explicit solution of (19) is not available. ◦

Due to the delay stemming from the time it takes to solve (19) for the sampled state χ, forward invariance of the set $\mathcal{R}$

along the closed-loop solutions of (16) with delayed sampled-data updates of $\rho^\star$ might be jeopardized. More specifically, consider the sampled state χ and a value $\rho \in \Phi$ satisfying $\chi \in \mathcal{E}_\rho(P)$, or equivalently,

$$g(\chi, \rho) := |\chi - A^\perp \rho|_P - \beta(\rho) \leq 0, \tag{21}$$

to simplify the notation. Imagine that it takes T seconds to compute $\rho^\star(\chi)$. During this time, since ρ is held constant in (13) and (16), Proposition 1 implies that the state x remains in the interior $\mathcal{E}_\rho(P)$ for all positive times, namely $g(x, \rho) < 0$. On the other hand it may happen that x does not belong to $\mathcal{E}_{\rho^\star(\chi)}(P)$, due to the dynamic evolution from χ to x over the T computation seconds.

Motivated by the above setting, we address below the question of selecting a "retraction" $\rho^+ = \pi(x, \rho, \rho_{\text{opt}})$ in such a way that

$$[g(\chi, \rho) \leq 0 \text{ and } g(x, \rho) \leq 0] \quad \Rightarrow \quad g(x, \rho^+) \leq 0, \tag{22}$$

where ρ_{opt} could be $\rho^\star(\chi)$ or any other (possibly suboptimal) candidate update for ρ, computed by an optimizer running for a sample-and-hold period T.

We call the set-valued map π a *retraction*, because it ensures that x is included in the ellipsoid $\mathcal{E}_{\rho^+}(P)$ by *retracting* ρ_{opt} in the direction of ρ, which satisfies $x \in \mathcal{E}_\rho(P)$ as stated in (22). Based on the assumption that $x \in \mathcal{E}_\rho(P)$, henceforth we focus on the set

$$\mathcal{E}_\rho(P) \times \Phi = \{(x, \rho) \in \overline{\mathcal{R}} \times \Phi : \ g(x, \rho) \leq 0\}. \tag{23}$$

We define π through a combination of two (retr)actions. The first one ensures feasibility, and the second one ensures optimality with respect to the distance of ρ^+ to the origin.

For the first retraction, termed the feasibility retraction, define $\mu(x, \rho, \rho_{\text{opt}}) \subset [0, 1]$, as

$$\mu(x, \rho, \rho_{\text{opt}}) := \begin{cases} \{0\} & \text{if } \begin{cases} g(x, \rho_{\text{opt}}) < 0 \\ g(x, \rho) \leq 0 \end{cases} \\ [0, 1] & \text{if } \begin{cases} g(x, \rho_{\text{opt}}) = 0 \\ g(x, \rho) = 0 \end{cases} \\ \left\{ \frac{g(x, \rho_{\text{opt}})}{g(x, \rho_{\text{opt}}) - g(x, \rho)} \right\} & \text{if } \begin{cases} g(x, \rho_{\text{opt}}) > 0 \\ g(x, \rho) \leq 0 \end{cases} \end{cases} \tag{24}$$

and, with a slight abuse of notation, define the *retracted* convex combination

$$\rho_\mu := \mu\rho + (1 - \mu)\rho_{\text{opt}} \qquad \text{for} \qquad \mu \in \mu(x, \rho, \rho_{\text{opt}}) \tag{25}$$

arbitrary. Under the assumption $(x, \rho) \in \mathcal{E}_\rho(P) \times \Phi$, the definition of $\mu(x, \rho, \rho_{\text{opt}})$ ensures feasibility (namely $x \in \mathcal{E}_{\rho_\mu}(P)$, for all $\mu \in \mu(x, \rho, \rho_{\text{opt}})$ as it will be stated and proven in Lemma 2, in Section III-C). Note that $\mu(x, \rho, \rho_{\text{opt}}) \subset [0, 1]$ since $g(x, \rho) \leq 0$ by assumption.

For the second retraction, called the optimality retraction, let $\mu \in \mu(x, \rho, \rho_{\text{opt}})$ arbitrary, and ρ_μ defined in (25). We further *retract* ρ_μ in the direction of ρ, by relying on the solution of the optimization problem

$$\begin{aligned} \nu_\mu^\star &:= \text{argmin}_{\nu \in [0,1]} \, |\nu\rho_\mu + (1 - \nu)\rho|^2 \\ &= \text{argmin}_{\nu \in [0,1]} \, |\nu(1 - \mu)(\rho_{\text{opt}} - \rho) + \rho|^2. \end{aligned} \tag{26}$$

If $\mu \neq 1$ and $\rho_{\text{opt}} \neq \rho$, the solution can be computed explicitly as

$$\nu_\mu^\star = \min \left\{ 1, \max \left\{ 0, \frac{1}{1 - \mu} \frac{(\rho - \rho_{\text{opt}})^\top \rho}{|\rho - \rho_{\text{opt}}|^2} \right\} \right\}. \tag{27}$$

The statement is made precise in Lemma 3 and proven in Section III-C. For $\mu = 1$ or $\rho_{\text{opt}} = \rho$, we simply define $\nu_\mu^\star = 0$. Finally, with

$$\mathcal{P} := \{\nu_\mu^\star(1 - \mu) \in [0, 1] : \ \mu \in \mu(x, \rho, \rho_{\text{opt}})\}, \tag{28}$$

the selection of the set-valued map π is completed by a further convex combination with $\mathcal{P}$, as follows[1]

$$\pi(x, \rho, \rho_{\text{opt}}) := \begin{cases} \mathcal{P} \cdot \{\rho_{\text{opt}} - \rho\} + \{\rho\}, & |x|_P > \beta(0), \\ \mathcal{P} \cdot \{\rho_{\text{opt}} - \rho\} + \{\rho\} \cup \{0\}, & |x|_P = \beta(0), \\ \{0\}, & |x|_P < \beta(0). \end{cases} \tag{29}$$

Remark 6: From (28) and (29) it is immediately clear why the selection of $\nu_\mu^\star$ in the case $\mu = 1$ or $\rho_{\text{opt}} = \rho$ is not important, since in these cases $\nu_\mu^\star$ is multiplied by zero. ∘

The following proposition establishes important properties of the *retraction* π in (29). Its proof is given next, in Section III-C, together with the above-mentioned lemmas.

Proposition 2: Let $(x, \rho, \rho_{\text{opt}}) \in \mathcal{E}_\rho(P) \times \Phi \times \mathbb{R}^p$. Then, the set-valued map $\pi : \mathcal{E}_\rho \times \Phi \times \mathbb{R}^p \rightrightarrows \Phi$ in (29) with $\rho^+ \in \pi(x, \rho, \rho_{\text{opt}})$ satisfies

$$|x - A^\perp \rho^+|_P \leq \beta(\rho^+) \quad \text{and} \quad |\rho^+| \leq |\rho|. \tag{30}$$

Moreover, π is outer semi-continuous. ⌟

For a definition of outer semi-continuity see [14, Definition 5.9], for example.

Remark 7: According to (30), the set-valued map (29) provides an update $\rho^+ \in \pi(x, \rho, \rho_{\text{opt}})$ such that $g(x, \rho^+) \leq 0$. Through a slight variation, i.e., by replacing (29) by

$$\pi_\varepsilon(x, \rho, \rho_{\text{opt}}) := \begin{cases} \mathcal{P} \cdot \{(1 - \varepsilon)(\rho_{\text{opt}} - \rho)\} + \{\rho\}, & |x|_P > \beta(0), \\ \mathcal{P} \cdot \{(1 - \varepsilon)(\rho_{\text{opt}} - \rho)\} + \{\rho\} \cup \{0\}, & |x|_P = \beta(0), \\ \{0\}, & |x|_P < \beta(0), \end{cases}$$

for some small $\varepsilon > 0$, and considering the update $\rho^+ \in \pi_\varepsilon(x, \rho, \rho_{\text{opt}})$, it can also be guaranteed that both $g(x, \rho^+) < 0$ and $|\rho^+| \leq |\rho|$ whenever

$$g(x, \rho) < 0 \quad \text{and} \quad |x|_P \neq \beta(0), \tag{31}$$

which follows from the convexity of Φ. ∘

C. Proof of Proposition 2

To prove Proposition 2, we first state and prove two lemmas that establish the properties of each of the two retractions described in the previous subsection. The first lemma establishes the properties of the retracted convex combination in (25).

Lemma 2: Let $(x, \rho, \rho_{\text{opt}}) \in \mathcal{E}_\rho(P) \times \Phi \times \mathbb{R}^p$. Then, for any $\mu \in \mu(x, \rho, \rho_{\text{opt}})$ the convex combination ρ_μ in (24), (25) satisfies $g(x, \rho_\mu) \leq 0$, namely $x \in \mathcal{E}_{\rho_\mu}(P)$. Moreover, $\mu : \mathcal{E}_\rho(P) \times \Phi \times \mathbb{R}^p \rightrightarrows [0, 1]$ is outer semi-continuous. ⌟

[1]Here, for $\mathcal{A}, \mathcal{B} \subset \mathbb{R}^n$ and $\mathcal{P} \subset \mathbb{R}$, we use the set operations $\mathcal{P} \cdot \mathcal{A} = \{p \cdot a \in \mathbb{R}^n : \ p \in \mathcal{P}, \ a \in \mathcal{A}\}$ and $\mathcal{A} + \mathcal{B} = \{a + b \in \mathbb{R}^n : \ a \in \mathcal{A}, \ b \in \mathcal{B}\}$.

Proof: Let $\mu \in \mu(x,\rho,\rho_{\text{opt}})$. If $g(x,\rho_{\text{opt}}) < 0$, then $\mu = 0$ and the statement follows directly from the definition of ρ_μ. Similarly, for $g(x,\rho_{\text{opt}}) = 0$ and $g(x,\rho) = 0$ it holds that

$$\mu g(x,\rho_{\text{opt}}) + (1-\mu) g(x,\rho) = 0 \qquad \forall\ \mu \in [0,1].$$

For $g(x,\rho_{\text{opt}}) > 0$ the definition of μ implies that $\mu = (0,1]$ and

$$\begin{aligned} g(x,\rho_\mu) &= g(x, \mu\rho + (1-\mu)\rho_{\text{opt}}) \\ &\leq \mu g(x,\rho) + (1-\mu) g(x,\rho_{\text{opt}}) \\ &= \tfrac{g(x,\rho_{\text{opt}})}{g(x,\rho_{\text{opt}}) - g(x,\rho)} g(x,\rho) + \tfrac{g(x,\rho_{\text{opt}}) - g(x,\rho) - g(x,\rho_{\text{opt}})}{g(x,\rho_{\text{opt}}) - g(x,\rho)} g(x,\rho_{\text{opt}}) \\ &= 0 \end{aligned}$$

where the inequality follows from the convexity of g.

From the definition of $\mu(\cdot)$, continuity of $\mu(\cdot)$ follows for all $(x,\rho,\rho_{\text{opt}}) \in \mathcal{E}_\rho(P) \times \Phi \times \mathbb{R}^p$ satisfying the additional properties $g(x,\rho_{\text{opt}}) \neq 0$ and $g(x,\rho) \neq 0$. Let $(x_i,\rho_i,\rho_{\text{opt}_i})_{i\in\mathbb{N}} \subset \mathcal{E}_{\rho_i}(P) \times \Phi \times \mathbb{R}^p$ denote an arbitrary sequence with the properties $(x_i,\rho_i,\rho_{\text{opt}_i}) \to (\bar{x},\bar{\rho},\bar{\rho}_{\text{opt}})$ for $i \to \infty$ and $g(\bar{x},\bar{\rho}_{\text{opt}}) = 0$, $g(\bar{x},\bar{\rho}) = 0$. Since the domain of $\mu(\cdot)$ is closed, it holds that $(\bar{x},\bar{\rho},\bar{\rho}_{\text{opt}}) \in \mathcal{E}_{\bar{\rho}}(P) \times \Phi \times \mathbb{R}^p$. Moreover, from the properties of the function g and the definition of $\mu(\cdot)$ it follows that

$$0 \leq \mu(x_i,\rho_i,\rho_{\text{opt}_i}) \leq 1, \quad \forall\ i \in \mathbb{N},$$

i.e., $\mu(x_i,\rho_i,\rho_{\text{opt}_i}) \in \mu(\bar{x},\bar{\rho},\bar{\rho}_{\text{opt}}) = [0,1]$ for all $i \in \mathbb{N}$, which shows that $\mu(\cdot)$ is outer semi-continuous. ■

The second lemma establishes the properties of the convex combination in (29). Interestingly, feasibility is guaranteed for any such convex combination (for any $\nu \in [0,\nu_\mu^\star]$), which shows a desirable robustness property.

Lemma 3: Let $(x,\rho,\rho_{\text{opt}}) \in \mathcal{E}_\rho(P) \times \Phi \times \mathbb{R}^p$, $\mu \in \mu(x,\rho,\rho_{\text{opt}})$ and define ρ_μ as in (25). Then $g(x,\nu\rho_\mu + (1-\nu)\rho) \leq 0$ for all $\nu \in [0,1]$. Moreover, for $\mu \neq 1$ and $\rho_{\text{opt}} \neq \rho$, the value $\nu_\mu^\star$ in (27) defines the unique solution of the optimization problem (26) and $\nu_\mu^\star$ depends continuously on μ, ρ and ρ_{opt}.

Proof: First note that Lemma 2 implies $g(x,\rho_\mu) \leq 0$ and $g(x,\rho) \leq 0$. Then inequality $g(x,\nu\rho_\mu + (1-\nu)\rho) \leq 0$ follows immediately from the convexity of $g(x,\cdot)$. For a fixed ρ_μ, optimality of $\nu_\mu^\star$ in (26) follows from direct calculations and existence and uniqueness of $\nu_\mu^\star$ follows from the strict convexity of the objective function and the compactness and the convexity of the set $[0,1]$. Similarly, continuity of $\nu_\mu^\star$ with respect to μ, ρ and ρ_{opt} follows from (26). ■

With Lemmas 2 and 3 we can finally prove Proposition 2.

Proof of Proposition 2: The properties in (30) follow from Lemma 2 and Lemma 3. Outer semi-continuity follows from the outer semi-continuity of $\mu(\cdot)$ established in Lemma 2 and the continuity of $\nu_\mu^\star$ discussed in Lemma 3.

In particular, an arbitrary sequence $(\mu_i,x_i,\rho_i,\rho_{\text{opt}_i})_{i\in\mathbb{N}} \subset [0,1] \times \mathcal{E}_{\rho_i}(P) \times \Phi \times \mathbb{R}^p$ with $\mu_i \in \mu(x_i,\rho_i,\rho_{\text{opt}_i})$ for all $i \in \mathbb{N}$ and $(\mu_i,\rho_i,\rho_{\text{opt}_i}) \to (\bar{\mu},\bar{\rho},\bar{\rho}_{\text{opt}}) \in [0,1] \times \Phi \times \mathbb{R}^p$ for $i \to \infty$ satisfies

$$\nu_{\mu_i}^\star (1-\mu_i)(\rho_{\text{opt}_i} + \rho_i) + \rho_i \to \nu_{\bar{\mu}}^\star (1-\bar{\mu})(\bar{\rho}_{\text{opt}} + \bar{\rho}) + \bar{\rho}$$

for $i \to \infty$. Thus, outer semi-continuity can be concluded from the definition of π in (29). Recall that we have defined $\nu_\mu^\star = 0$ for $\mu = 1$ or $\rho_{\text{opt}} = \rho$, as justified in Remark 6. ■

IV. Closed-loop analysis based on a hybrid system formulation

In the following, we construct a stabilizing feedback law combining the closed-loop dynamics (16) with a discrete update of ρ through (29). Our solution relies on the properties discussed and the definitions introduced in Section III, stemming from the optimization problem (19). Starting with $x(0)$ such that (19) is feasible, we investigate the sampled-data closed-loop dynamics using a hybrid systems formalism [14].

A. A hybrid systems formulation

To describe the overall closed-loop dynamics in the form of a hybrid system, we consider the augmented state $\xi = (x,\chi,\rho,\tau) \in \overline{\Xi}$, where $\overline{\Xi}$ is the closure of the set

$$\Xi := \mathcal{E}_\rho(P) \times \mathcal{E}_\rho(P) \times \text{int}(\Phi) \times [0,\overline{\tau}], \tag{32}$$

with $\overline{\tau} \in \mathbb{R}_{>0}$. Here, x is the state of plant (3) and χ is a sample-and-hold version of x at certain sampling instances. Moreover, $\rho \in \Phi$ defines an induced equilibrium pair $(x_e,u_e) = (A^\perp\rho, B^\perp\rho) \in \Gamma$ (see (5b)). Finally, τ is used to trigger discrete-time updates based on lower and upper bounds $\underline{\tau},\overline{\tau} \in \mathbb{R}_{>0}$ satisfying $\underline{\tau} \leq \overline{\tau}$. In particular, with $\underline{\tau}$ and $\overline{\tau}$, the flow and the jump sets are defined as

$$\mathcal{C} = \overline{\Xi}, \qquad \mathcal{D} = \mathcal{E}_\rho(P) \times \mathcal{E}_\rho(P) \times \Phi \times [\underline{\tau},\overline{\tau}], \tag{33}$$

respectively. The continuous dynamics is selected as

$$\dot{\xi} = \begin{bmatrix} \dot{x} \\ \dot{\chi} \\ \dot{\rho} \\ \dot{\tau} \end{bmatrix} = F(\xi) := \begin{bmatrix} f(x,k(x,\rho)) \\ 0 \\ 0 \\ 1 \end{bmatrix}, \ \xi \in \mathcal{C} \tag{34a}$$

where f and k are defined in (16) and (13), respectively. Finally, the jump map is defined as

$$\xi^+ = \begin{bmatrix} x^+ \\ \chi^+ \\ \rho^+ \\ \tau^+ \end{bmatrix} \in G(\xi) := \begin{bmatrix} x \\ x \\ \pi(x,\rho,\rho^\star(\chi)) \\ 0 \end{bmatrix}, \ \xi \in \mathcal{D}, \tag{34b}$$

where the "retraction" π defined in (29) describes the update of the shifting parameter ρ, and $\rho^\star$ defines the optimal solution of (19).

Note that $\rho^\star$ only depends on the quantity χ, which remains constant along flowing solutions. Thus, $\rho^\star(\chi)$ can be evaluated before the jump time occurs as long as the time required to compute the optimal solution of (19) can be upper bounded by $\overline{\tau}$. Since the optimization problem (19) is convex, according to the properties established in Lemma 1, the function $\rho^\star(\cdot)$ can be evaluated efficiently by solving a convex optimization problem. While the computation of $\rho^\star(\chi)$ might be expensive, the time to evaluate π is computationally cheap by construction. This structure is clarified in Figure 1, where the evaluation of π is instantaneous, while the evaluation of $\rho^\star(\cdot)$ may require any computation time $\tau \in [\underline{\tau},\overline{\tau}]$.

Remark 8: Note that the definition of Ξ in (32), with a slight abuse of notation, uses the Cartesian product even though $\mathcal{E}_\rho(P)$ depends on $\rho \in \Phi$, and thus the shape of Ξ is non-trivial. ∘

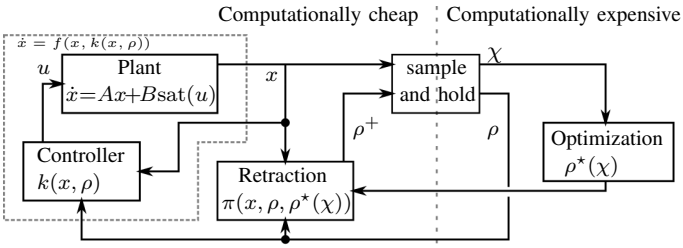

Fig. 1. Main components of the hybrid closed loop (34). The overall system can be split in continuous-time dynamics and discrete-time dynamics. The discrete time update through the optimization problem (19) may be computationally expensive, while the rest of the components are computationally cheap.

Before we analyze and prove properties of the hybrid closed-loop system (34), we point out that the hybrid system is well posed [14] and its solutions enjoy desirable properties.

Lemma 4: The hybrid system (34) satisfies the hybrid basic conditions of [14, Assumption 6.5]. Moreover, all maximal solutions are complete and have domains that are unbounded in the $t \in \mathbb{R}_{\geq 0}$ and $j \in \mathbb{N}$ directions. ⌟

Proof: The first statement follows immediately from the fact that f and k (see (16) and (12)) are continuous, the fact that π is outer semi-continuous (see Proposition 2) and the fact that $\mathcal{C}$ and $\mathcal{D}$ are closed.

To prove completeness of maximal solutions, first note that the selection and the properties of the feedback law $k(x,\rho)$ and the properties of the update $\rho^\star$ of ρ ensure forward invariance of $\overline{\Xi}$ for the hybrid closed-loop (34). Then, the viability condition [14, Prop. 6.10] holds and completeness of solutions follows from standard arguments. Finally, from the definitions of the flow and jumps sets through $\underline{\tau}, \overline{\tau} \in \mathbb{R}_{>0}$ it holds that two consecutive jumps of any solution are separated by at least $\underline{\tau}$ and at most $\overline{\tau}$ units of flowing time. This last observation means that all solutions enjoy uniform direct and reverse dwell-time properties, namely their domains are unbounded both in the t and the j directions. ■

A solution of the hybrid system (34) evolves in the state-space $\overline{\Xi}$ (see (32)) with hybrid time domain $\mathrm{dom}(\xi) \subset \mathbb{R}_{\geq 0} \times \mathbb{N}$, see [14, Definition 2.3]. With a slight abuse of notation, since the x-component of each hybrid solution remains constant across jumps, according to the jump map (34b), we use the notation $x(t)$, $t \in \mathbb{R}_{\geq 0}$ and $x(t,j)$, $(t,j) \in \mathrm{dom}(\xi)$ interchangeably. Thus, $x(\cdot) : \mathbb{R}_{\geq 0} \to \mathbb{R}^n$ is well defined according to Lemma 4 and absolutely continuous due to the properties of the feedback law $k(x,\rho)$.

B. Closed loop analysis of the hybrid system

In this section we derive the stability properties of the hybrid closed-loop system (34). To this end, for $\overline{\tau} > 0$, we introduce the compact set

$$\mathcal{A} = \{0\} \times \{0\} \times \{0\} \times [0, \overline{\tau}] \subset \Xi, \tag{35}$$

which captures the desired asymptotic behavior of the plant-controller states (i.e., all of them should be zero) without imposing any specific requirement on the timer τ.

Theorem 1: Consider the hybrid system (34) where π is defined in (29) and $\rho^\star(\cdot)$ denotes the optimizer of (19). Moreover, let $0 < \underline{\tau} \leq \overline{\tau}$ be arbitrary. Then, the set $\mathcal{A}$ in (35) is asymptotically stable. Moreover, the set $\Xi \subset \overline{\Xi}$ in (32) is forward invariant and contained in the region of attraction of $\mathcal{A}$. ⌟

The proof of this main result is postponed to the end of this section and relies on the properties established in Proposition 3 discussed next.

Proposition 3: Consider the hybrid system (34) where π is defined in (29) and $\rho^\star(\cdot)$ denotes the optimizer of (19). Moreover, let $0 < \underline{\tau} \leq \overline{\tau}$ be arbitrary.

For any initial condition $\xi \in \Xi$ (as per (32)), all the ensuing solutions are such that

1) $\rho(t,j) \in \mathrm{int}(\Phi)$ for all $(t,j) \in \mathrm{dom}(\xi)$;
2) $g(x(t,j), \rho(t,j)) \leq 0$ for all $(t,j) \in \mathrm{dom}(\xi)$;
3) there exists $(T,J) \in \mathrm{dom}(\xi)$ such that $\rho(T,J) = 0$ and $g(x(T,J),0) \leq 0$; and
4) $|x(t,j)| \to 0$ for $(t,j) \to \infty$. ⌟

Note that initial conditions $\xi_0 \in \overline{\Xi} \backslash \Xi$ need to be excluded in Proposition 3 due to the discussion given in Remark 4.

Proof: Item 1. The condition $\rho_0 \in \mathrm{int}(\Phi)$ ensures that $\rho^\star(\chi(t,j)) \in \mathrm{int}(\Phi)$ for all $(t,j) \in \mathrm{dom}(\xi)$. Thus, the first statement follows immediately from the convexity of the set Φ together with the definition of the function π and the parameter $\nu_\mu^\star$ updating ρ through a convex combination, thus ensuring that $\mathrm{int}(\Phi)$ is not left.

Item 2. The second statement follows from the definition of the control law (13) stabilizing the reference point $x_e(\rho) = A^\perp \rho$ and the properties of the function π, established in (30) in Proposition 2.

Item 3. From the definition of π and in particular from Proposition 2, it follows that $|\rho(t,j)|$ is monotonically decreasing (but not necessarily strictly monotonically decreasing). Since $\rho(t,j)$ is only updated at discrete time steps, we use the notation $\rho(j)$ for simplicity in the following. Since $\overline{\tau} \in \mathbb{R}_{>0}$, it holds that $j \to \infty$ whenever $(t,j) \in \mathrm{dom}(\xi)$, $(t,j) \to \infty$.

Due to the monotonicity of $|\rho(j)| \geq 0$, the sequence $|\rho(j)|$ is convergent and, since $\rho(j)$ is bounded, there exists a convergent subsequence $\rho(j_k)$, $k \in \mathbb{N}$, satisfying $\rho(j_k) \to \rho^\#$ for $k \to \infty$, and $\rho^\#$ denotes an accumulation point of $\rho(j)$ (in view of the Bolzano-Weierstrass theorem).

To show that $(\rho(j))_{j\in\mathbb{N}}$ converges, by contradiction, we assume that $(\rho(j))_{j\in\mathbb{N}}$ has multiple accumulation points $\rho^{\#_1} \neq \rho^{\#_2}$. However, the existence of multiple accumulation points is a contradiction to the update of ρ defined through the function π in Proposition 2 and in particular the selection of $\nu_\mu^\star$ in Lemma 3, which is unique. We can thus conclude that $(\rho(j))_{j\in\mathbb{N}}$ is converging, i.e., there exists $\rho^\#$ such that $\rho(j) \to \rho^\#$ for $j \to \infty$.

According to Remark 2, it holds that

$$\begin{aligned}(x(t,j) - x_e(\rho(t,j)))^\top P f(x(t,j), k(x(t,j),\rho(t,j))) \\ \leq -\alpha |x(t,j) - x_e(\rho(t,j))|_P^2\end{aligned}$$

for almost all $(t,j) \in \mathrm{dom}(\xi)$. (In the following we drop the

time argument for simplicity of notation.) Moreover, with

$$\begin{aligned}&(x-A^\perp\rho^\#)^\top Pf(x,k(x,\rho))\\&-(\rho-\rho^\#)^\top(A^\perp)^\top Pf(x,k(x,\rho))\\&\qquad=(x-A^\perp\rho)^\top Pf(x,k(x,\rho))\end{aligned}$$

and

$$-\alpha|x-A^\perp\rho|_P^2\le-\alpha|x-A^\perp\rho^\#|_P^2+\alpha\|A^\perp\||\rho-\rho^\#|_P^2$$

it holds that

$$\begin{aligned}&(x-A^\perp\rho^\#)^\top Pf(x,k(x,\rho))\le-\alpha|x-A^\perp\rho^\#|_P^2\\&+\alpha\|A^\perp\||\rho-\rho^\#|_P^2+(\rho-\rho^\#)^\top(A^\perp)^\top Pf(x,k(x,\rho)).\end{aligned}\tag{36}$$

As a next step, we observe that $\mathcal{E}_\rho(P)$ is bounded for all $\rho\in\Phi$. Moreover, by construction $x(t,j)\in\mathcal{E}_{\rho(t,j)}(P)$ for all $(t,j)\in\operatorname{dom}(\xi)$ and $|\rho(t,j)|$ is monotonically decreasing. This implies that

$$M(x_0,\rho_0):=\sup_{x\in\mathcal{E}_\rho(P),\ |\rho|\le|\rho_0|,\ u\in[-u^-,u^+]}|f(x,k(x,\rho))|<\infty.$$

We can continue with the estimate (36) and for almost all $(t,j)\in\operatorname{dom}(\xi)$ it holds that

$$\begin{aligned}&\tfrac{1}{2}\tfrac{d}{dt}V_{\rho^\#}(x)=(x-A^\perp\rho^\#)^\top Pf(x,k(x,\rho))\\&\le-\alpha|x-A^\perp\rho^\#|_P^2+c_1|\rho-\rho^\#|^2+c_2M(x_0,\rho_0)|\rho-\rho^\#|\end{aligned}$$

for appropriately selected $c_1,c_2\in\mathbb{R}_{>0}$. This implies that there exist $\kappa\in\mathcal{KL}$ and $\gamma\in\mathcal{K}$ such that

$$\begin{aligned}&|x(t,j)-A^\perp\rho^\#|\\&\quad\le\kappa(|x(t,j)-A^\perp\rho^\#|,t)+\gamma(\|\rho(t,j)-\rho^\#\|_{\mathcal{L}_\infty})\end{aligned}\tag{37}$$

(i.e., the system is input-to-state stable with respect to "disturbances" $\rho(t,j)-\rho^\#$). From inequality (37) together with the fact that $x(t,j)$ is bounded and $\rho(t,j)\to\rho^\#$ for $t\to\infty$, it follows that $x(t,j)\to A^\perp\rho^\#$ for $(t,j)\to\infty$.

As a last step we need to show that $\rho^\#=0$. In this context, note that $\rho^\#\neq0$ combined with $x(t,j)\to A^\perp\rho^\#$ for $(t,j)\to\infty$ leads to a contradiction with respect to the update of $\rho(t,j)$ defined through the function π defined in Proposition 2. Moreover, from $x(t,j)\to0$ for $(t,j)\to\infty$, the existence of $(T,J)\in\operatorname{dom}(\xi)$ with $|x(T,J)|\le\beta(0)$ follows. Thus, $\rho(t,j)=0$ is satisfied in finite time.

Item 4. This item follows immediately from the proof of item 3. ∎

With the properties established in Proposition 3 we are in the position to show asymptotic stability of $\mathcal{A}$. We emphasize that due to the well-posedness conditions proved in Lemma 4, the established asymptotic stability property is intrinsically robust and equivalent to a robust $\mathcal{KL}$ stability property of $\mathcal{A}$, due to the results in [14, Chapter 7].

Proof of Theorem 1: We prove asymptotic stability of $\mathcal{A}$ by first proving Lyapunov stability and then local convergence for all solutions starting in Ξ.

For Lyapunov stability, we use the ε-δ-criterion and we start by defining three constants, $c_1=\min\left\{1,\|A^\perp\|_2^{-1}\right\}$,

$$c_2=\min\left\{1,\tfrac{1}{\sqrt{\lambda_{\max}(P)}}\right\},\qquad c_3=\min\left\{1,\sqrt{\lambda_{\min}(P)}\right\},$$

which satisfy $c_1,c_2,c_3\in(0,1]$ by definition. Moreover, observe that the estimate

$$|x_e(\rho)|^2=\rho^\top(A^\perp)^\top A^\perp\rho\le\|A^\perp\|_2^2\rho^\top\rho$$

holds for all $\rho\in\Phi$ and $\|A^\perp\|_2>0$ since $B\neq0$ and thus $A^\perp\neq0$. As a next step, let $\bar\varepsilon\in(0,1)$ be arbitrary and let $\xi_0\in\Xi$ satisfy

$$|\xi_0|_{\mathcal{A}}\le\tfrac{\bar\varepsilon c_1c_2c_3}{16}\beta(0).$$

Then, the individual components of ξ_0 satisfy

$$\begin{aligned}|x_0|&\le\tfrac{\bar\varepsilon c_1c_2c_3}{16}\beta(0)\le\tfrac{\bar\varepsilon c_2c_3}{16}\beta(0),\\|\chi_0|&\le\tfrac{\bar\varepsilon c_1c_2c_3}{16}\beta(0)\le\tfrac{\bar\varepsilon c_2c_3}{16}\beta(0),\\|\rho_0|&\le\tfrac{\bar\varepsilon c_1c_2c_3}{16}\beta(0)\le\tfrac{\bar\varepsilon c_2c_3}{16}\beta(0),\end{aligned}$$

and the last inequality together with the definition of c_1 imply

$$|x_e(\rho_0)|\le\|A^\perp\|_2|\rho_0|\le\tfrac{\bar\varepsilon c_2c_3}{16}\beta(0).$$

Moreover, these inequalities together with $x^\top Px\le\lambda_{\max}(P)$ imply that

$$\begin{aligned}|x_e(\rho_0)|_P&\le\sqrt{\lambda_{\max}(P)}|x_e(\rho_0)|\le\tfrac{\bar\varepsilon c_3}{16}\beta(0),\\|x_0-x_e(\rho_0)|_P&\le\sqrt{\lambda_{\max}(P)}|x_0-x_e(\rho_0)|\le\tfrac{\bar\varepsilon c_3}{8}\beta(0).\end{aligned}\tag{38}$$

Note that

$$\begin{aligned}&\{x\in\mathbb{R}^n:|x-x_e(\rho_0)|_P\le\tfrac{\bar\varepsilon c_3}{8}\beta(0)\}\\&\qquad\subset\{x\in\mathbb{R}^n:\ |x|_P-|x_e(\rho_0)|_P\le\tfrac{\bar\varepsilon c_3}{8}\beta(0)\}\\&\qquad\subset\{x\in\mathbb{R}^n:\ |x|_P\le\tfrac{\bar\varepsilon c_3}{4}\beta(0)\}\subset\mathcal{E}_0(P),\end{aligned}$$

where the last inclusion holds in view of (38). Based on the definition and the properties of the closed-loop dynamics (34), $|\rho(t,j)|$ is decreasing for all $(t,j)\in\operatorname{dom}(\xi)$ and the x- and χ-components satisfy $|x(t,j)|_P\le\tfrac{\bar\varepsilon c_3}{4}\beta(0)$ and $|\chi(t,j)|_P\le\tfrac{\bar\varepsilon c_3}{4}\beta(0)$ for all $(t,j)\in\operatorname{dom}(\xi)$ since ρ jumps to $\rho^+=0$ at the first discrete-time step.

Using $\lambda_{\min}(P)x^\top x\le x^\top Px$, we can conclude that

$$\begin{aligned}|\xi(t,j)|_{\mathcal{A}}&\le|x(t,j)|+|\chi(t,j)|+|\rho(t,j)|\\&\le\tfrac{1}{\sqrt{\lambda_{\min}(P)}}(|x(t,j)|_P+|\chi(t,j)|_P)+|\rho(t,j)|\\&\le\tfrac{2}{\sqrt{\lambda_{\min}(P)}}\tfrac{\bar\varepsilon c_3}{4}\beta(0)+\tfrac{\bar\varepsilon c_2c_3}{16}\beta(0)\\&\le\tfrac{1}{2}\bar\varepsilon\beta(0)+\tfrac{\bar\varepsilon}{16}\beta(0)\le\bar\varepsilon\beta(0).\end{aligned}$$

Thus, for all $\varepsilon\in[0,\beta(0))]$, there exists $\delta(\varepsilon)=\tfrac{c_1c_2c_3}{16}\varepsilon$ such that $|\xi_0|_{\mathcal{A}}\le\delta(\varepsilon)$ implies $|\xi(t,j)|_{\mathcal{A}}\le\varepsilon$ for all $(t,j)\in\operatorname{dom}(\xi)$, which concludes the proof of Lyapunov stability.

Convergence to $\mathcal{A}$ for any solution starting in the set Ξ follows immediately from items 3 and 4 of Proposition 3, the fact that χ is a sampled version of x and the persistent jumping properties induced by the timeout quantity $\bar\tau$. ∎

Remark 9: Theorem 1 guarantees asymptotic stability of $\mathcal{A}$ defined in (35) with ERA Ξ for the hybrid closed loop (34). While one may expect the actual region of attraction to be larger than Ξ, a possible difficulty arises from the fact that the update function $\rho^\star(\chi)$ for the controller state ρ^+ is only defined for $\chi\in\overline{\mathcal{R}}$, i.e., the jump map (34b) cannot even be evaluated outside this set. We consider a heuristic extension of (34) that is defined on the larger flow and jump sets $\widehat{\mathcal{C}}=$

$\mathbb{R}^{2n} \times \Phi \times [0, \overline{\tau}]$ and $\widehat{\mathcal{D}} = \mathbb{R}^{2n} \times \Phi \times [\underline{\tau}, \overline{\tau}]$ and it provides a simple way to initialize $k(x, \rho)$ outside the set Ξ. While the flow map remains unchanged, we consider the following augmented version of optimization problem (19) to adapt the jump map:

$$\begin{aligned} \tilde{\rho}_c^\star(\chi) \in \operatorname{argmin}_\delta \; & s \\ \text{subject to } \; & |\chi - A^\perp \delta|_P \leq c\beta(\delta) + s, \\ & -\underline{u} \leq B^\perp \delta \leq \overline{u}, \quad s \geq 0. \end{aligned} \tag{39}$$

Here, $s \geq 0$ is a slack variable and $c \in (0, 1)$ denotes a parameter. We replace (34b) by

$$\xi^+ = \begin{bmatrix} x^+ \\ \chi^+ \\ \rho^+ \\ \tau^+ \end{bmatrix} \in \tilde{G}(\xi) := \begin{bmatrix} x \\ x \\ \tilde{\rho}_c^\star(\chi) \\ 0 \end{bmatrix}, \; \xi \in \widehat{\mathcal{D}} \tag{40}$$

in (34) and the optimization problem (39) is feasible by design. If $s^\star(\chi) = 0$ for $c \in (0, 1)$, then $(\chi, \rho^+) \in \mathcal{R} \times \operatorname{int}(\Phi)$. Thus, if at any point, along a solution, we obtain $g(x^+, \rho^+) < 0$, then we can replace (40) with the original jump map (34b) and continue with the dynamics (34). ◦

V. Controller Design through Inaccurate Solutions of (19)

The controller discussed in Section IV relies on the availability of the computationally expensive solution $\rho^\star(\cdot)$ of the optimization problem (19). In this section we relax this assumption and investigate the properties of an extended hybrid closed loop relying on inaccurate solutions of (19), which are computationally cheaper.

A. An extended hybrid system formulation

We extend the hybrid dynamics (34) by considering an additional state $r \in \mathbb{R}^p$ and thus define $\xi_r = (x, \chi, \rho, r, \tau) \in \overline{\Xi}_r$, where $\overline{\Xi}_r$ is the closure of the set

$$\Xi_r := \mathcal{E}_\rho(P) \times \mathcal{E}_\rho(P) \times \operatorname{int}(\Phi) \times \operatorname{int}(\Phi) \times [0, \overline{\tau}], \tag{41}$$

paralleling the definition in (32). Accordingly, the flow set and the jump set are defined as

$$\mathcal{C}_r = \overline{\Xi}_r \quad \text{and} \quad \mathcal{D}_r = \mathcal{E}_\rho(P) \times \mathcal{E}_\rho(P) \times \Phi \times \Phi \times [\underline{\tau}, \overline{\tau}].$$

The corresponding closed-loop dynamics is

$$\dot{\xi}_r = \begin{bmatrix} \dot{x} \\ \dot{\chi} \\ \dot{\rho} \\ \dot{r} \\ \dot{\tau} \end{bmatrix} = F_r(\xi) := \begin{bmatrix} f(x, k(x, \rho)) \\ 0 \\ 0 \\ 0 \\ 1 \end{bmatrix}, \; \xi_r \in \mathcal{C}_r, \tag{42a}$$

$$\xi_r^+ = \begin{bmatrix} x^+ \\ \chi^+ \\ \rho^+ \\ r^+ \\ \tau^+ \end{bmatrix} \in G_r(\xi) := \begin{bmatrix} x \\ x \\ \pi_\varepsilon(x, \rho, r^+) \\ \omega(\chi, \rho, r) \\ 0 \end{bmatrix}, \; \xi_r \in \mathcal{D}_r, \tag{42b}$$

where $\omega : \mathbb{R}^n \times \Phi \times \Phi \rightrightarrows \mathbb{R}^p$ denotes an outer semi-continuous and locally bounded set-valued map. Here, ω replaces the optimizer $\rho^\star(\chi)$ in π_ε. Outer semi-continuity and local boundedness are necessary to ensure that the hybrid basic conditions [14, Assumption 6.5] are satisfied, i.e., Lemma 4 is also applicable to (42). Additionally, note that we have replaced the retraction π by π_ε introduced in Remark 7. The function π_ε instead of π is used to guarantee $\rho^+ \in \operatorname{int}(\Phi)$ which held before due to optimality of $\rho^\star(\chi)$, whereas r^+ is not necessarily optimal in this extended scheme. The diagram representing the dynamics (42) is shown in Figure 2. The

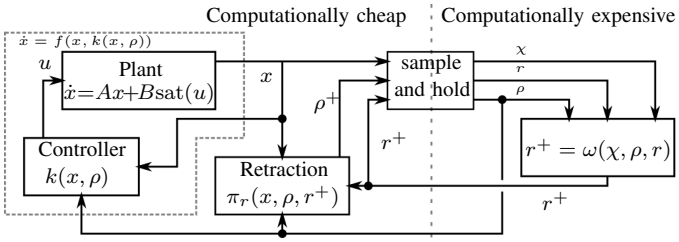

Fig. 2. Visualization of the extended closed-loop dynamics of the hybrid system (42). The diagram extends the setting in Figure 1.

dynamics (42) can be globally initialized through the ideas discussed in Remark 9, if necessary.

To state a result similar to Proposition 3 and Theorem 1, we assume that the set-valued map ω satisfies the following property.

Property 1: For all $(\chi, r^0) \in \mathcal{E}_{r^0}(P) \times \Phi$, an arbitrary sequence $(r^k)_{k \in \mathbb{N}} \subset \Phi$ defined through the set valued map $\omega : \mathcal{E}_\rho(P) \times \Phi \times \Phi \rightrightarrows \Phi$,

$$r^{k+1} \in \omega(\chi, \rho, r^k), \qquad r^0 \in \Phi, \tag{43}$$

converges to some $r^\# \in \Phi$ as $k \to \infty$. Moreover, the sequence and the limit satisfy $g(\chi, r^k) \leq 0$ for all $k \in \mathbb{N}$ and

$$|r^\# - \rho^\star(\chi)| \leq \tfrac{1}{2} \frac{\sqrt{\lambda_{\min}(P)}}{\|A^\perp\|} \beta(\rho^\star(\chi)). \tag{44}$$

◇

Together with $|A^\perp r^\# - A^\perp \rho^\star(\chi)| \leq \|A^\perp\| |r^\# - \rho^\star(\chi)|$, condition (44) implies that

$$A^\perp r^\# \in \operatorname{int}(\mathcal{E}_{\rho^\star(\chi)}(P)).$$

In particular, even if $A^\perp r^\#$ is asymptotically stabilized instead of $A^\perp \rho^\star(\chi)$, the proximity between $A^\perp r^\#$ and $A^\perp \rho^\star(\chi)$ implies that $r^\#$ is pulled towards the origin. Once $x_e(r^\#) = A^\perp r^\# \in \mathcal{E}_0(P)$ and $x(t, j)$ converges to $x_e(r^\#)$, the shifting parameter is updated through $\rho^+ = 0$, according to the definition of π_ε. Note that the scalar $\frac{1}{2}$ at the right-hand side of (44) is arbitrary and can be replaced by any number in the interval $[0, 1)$.

In the next subsection we give an example of a function ω satisfying Property 1 and stemming from an interior point algorithm. We conclude this section by extending Proposition 3 and Theorem 1 to the hybrid dynamics (42).

Proposition 4: Consider the hybrid system (42) where π_ε is defined in Remark 7 for some $\varepsilon \in (0, 1)$, and ω is outer semi-continuous, locally bounded and satisfies Property 1. Additionally, let $0 < \underline{\tau} \leq \overline{\tau}$ be arbitrary.

For any initial condition $\xi_r \in \Xi_r$ (as per (41)), all the ensuing solutions are such that

1) $\rho(t,j) \in \operatorname{int}(\Phi)$ for all $(t,j) \in \operatorname{dom}(\xi_r)$;
2) $g(x(t,j), \rho(t,j)) \leq 0$ for all $(t,j) \in \operatorname{dom}(\xi_r)$;
3) there exists $(T,J) \in \operatorname{dom}(\xi_r)$ such that $\rho(T,J) = 0$ and $g(x(T,J),0) \leq 0$; and
4) $|x(t,j)|_P \to 0$ for $(t,j) \to \infty$. ⌟

Theorem 2: Consider the hybrid system (42) where π_ε for $\varepsilon \in (0,1)$ is defined in Remark 7 and ω is outer semi-continuous, locally bounded and satisfies Property 1. Moreover, let $0 < \underline{\tau} \leq \overline{\tau}$ be arbitrary. Then, the set

$$\mathcal{A}_r := \{0\} \times \{0\} \times \{0\} \times \{\omega(0,0,r) | r \in \Phi\} \times [0, \overline{\tau}]$$

is asymptotically stable. Moreover, the set $\Xi_r \subset \overline{\Xi}_r$ is forward invariant and contained in the region of attraction of $\mathcal{A}_r$. ⌟

Proof of Proposition 4: Item 1. The first statement follows again from the convexity of Φ together with the properties of π_ε and $\nu_\mu^\star$. Here, the function π_ε (defined in Remark 7) instead of the function π ensures that $\rho^+ \in \operatorname{int}(\Phi)$. Note that the parameter ε is not necessary in the proof of Proposition 3 since $\rho^\star(\chi)$ is in the interior of Φ for all $\chi \in \mathcal{R}$ (according to Lemma 1), while r^+ might be on the boundary of Φ. In particular, in Proposition 3, ρ^+ is a convex combination of $\rho \in \operatorname{int}(\Phi)$ and $\rho^\star(\chi) \in \operatorname{int}(\Phi)$, i.e., $\rho^+ \in \operatorname{int}(\Phi)$. Here, $r^+ \in \Phi$ and $\rho \in \operatorname{int}(\Phi)$ and the set-valued map π_ε ensures that $\rho^+ \in \operatorname{int}(\Phi)$.

Item 2. Note that the second item only depends on the definition of the control law (13) and the definition of the function π replaced by π_ε, i.e., the result follows exactly the same lines as the proof of Proposition 3, item 2.

Item 3. Convergence of $\rho(t,j) \to \rho^\# \in \mathbb{R}^p$ for $(t,j) \to \infty$ as well as convergence $x(t,j) \to A^\perp \rho^\#$ for $(t,j) \to \infty$ follows the same arguments as in the proof of Theorem 3, item 2. The fact that $\rho^\# = 0$ follows from the property $x(t,j) \to A^\perp \rho^\#$ for $(t,j) \to \infty$, the properties (43)-(44) and the selection of the update $\rho(t,j)$. Moreover, from $x(t,j) \to 0$ for $(t,j) \to \infty$ the existence of $(T,J) \in \operatorname{dom}(\xi_r)$ with $|x(T,J)| \leq \beta(0)$ follows. Thus, $\rho(t,j) = 0$ is satisfied in finite time.

Item 4. As in the proof of Proposition 3, item 4 follows immediately from items 2 and 3. ■

Proof of Theorem 2: The statement follows from similar ideas to the ones used in the proof of Theorem 1. ■

B. The function ω, a logarithmic barrier method example

In this section we discuss a possible implementation of ω satisfying Property 1 in terms of a logarithmic barrier method where we follow the notation in [9, Chapter 11] for the derivation. Thus, instead of using a black-box optimization algorithm to evaluate $\rho^\star(\cdot)$, as in Section IV, we discuss here a possible explicit implementation of $\omega(\cdot,\cdot,\cdot)$, which is computationally cheaper.

To this end, as a first step, we rewrite the optimization problem (19) in the form

$$\begin{aligned} &\operatorname{argmin}_\delta \;\; h_0(\delta;\chi) \\ &\text{subject to} \;\; h_i(\delta;\chi) \leq 0, \qquad i = 1,\dots,d, \end{aligned} \tag{45}$$

$d \in \mathbb{N}$, where $h_i : \mathbb{R}^n \to \mathbb{R}$ are twice continuously differentiable for all $i \in \{0,\dots,d\}$.

Continuous differentiability does not directly hold for the construction in (19) because $g(\chi,\cdot)$ is not continuously differentiable. Nevertheless, due to the convexity of the norm, the concavity of β, and the positivity of β on the domain Φ, the conditions $g(\chi,\delta) \leq 0$ and $\delta \in \Phi$ in (19), (21) are equivalent to

$$\begin{aligned} h_j(\delta;\chi) &:= |\chi - A^\perp \delta|_P^2 - (u_j^- + B_{j,:}^\perp \delta)^2 \leq 0, \\ h_{j+m}(\delta;\chi) &:= |\chi - A^\perp \delta|_P^2 - (u_j^+ - B_{j,:}^\perp \delta)^2 \leq 0, \\ h_{j+2m}(\delta;\chi) &:= -u_j^- - B_{j,:}^\perp \delta \leq 0, \\ h_{j+3m}(\delta;\chi) &:= -u_j^+ + B_{j,:}^\perp \delta \leq 0, \end{aligned}$$

for all $j = 1,\dots,m$, where $B_{j,:}^\perp$ denotes the jth row of $B^\perp$. By additionally identifying $h_0(\delta;\chi) = |\delta|^2$ and $d = 4m$, the convex optimization problem (45) is an alternative representation of (19).

To compute an approximation of the optimal solution of (45) using the logarithmic barrier method, we define the function

$$\phi(\delta;\chi) = -\textstyle\sum_{j=1}^r \log(-h_j(\delta;\chi))$$

and, for a parameter $\ell \in \mathbb{R}_{>0}$, we approximate the optimization problem (45) through

$$\rho^{\#_\ell}(\chi) = \operatorname{argmin}_\delta \; h_0(\delta;\chi) + \tfrac{1}{\ell}\phi(\delta;\chi). \tag{46}$$

For $\ell \to \infty$, it holds that $\rho^{\#_\ell}(\chi) \to \rho^\star(\chi)$ and in particular the estimate

$$0 \leq |\rho^{\#_\ell}(\chi)|^2 - |\rho^\star(\chi)|^2 \leq \tfrac{d}{\ell} \tag{47}$$

is satisfied [9, Chapter 11.3].

Moreover, under the assumption that r^k, $k \in \mathbb{N}$, satisfies $h_i(r^k;\chi) < 0$ for a fixed $\chi \in \mathcal{R}$ and for all $i \in \{1,\dots,d\}$, we may select ω satisfying Property 1 by choosing

$$r^{k+1} = r^k + \alpha r_\Delta.$$

Here, r_Δ denotes the solution of a Newton step

$$\begin{aligned} &\left[\ell \nabla_\delta^2 h_0(r^k;\chi) + \nabla_\delta^2 \phi(r^k;\chi)\right] r_\Delta \\ &\qquad = \left[\ell \nabla_\delta h_0(r^k;\chi) + \nabla_\delta \phi(r^k;\chi)\right] \end{aligned}$$

and $\alpha \in (0,1)$ denotes a small enough stepsize such that r^{k+1} is again strictly feasible, i.e., $h_i(r^{k+1};\chi) < 0$ for all $i \in \{1,\dots,d\}$. Based on this idea, we can define the update $r^+ = \omega(\chi,\rho,r)$ through Algorithm 1.

Step 1 in Algorithm 1 is necessary to ensure that $\chi \in \operatorname{int}(\mathcal{E}_\rho(P))$ satisfies $\chi \in \operatorname{int}(\mathcal{E}_{r^0}(P))$. Once a strictly feasible r^0 is found, i.e., $g(\chi,r^0) < 0$ is satisfied, $\kappa \in \mathbb{N}$ Newton steps are performed to update r. Since $g(\chi,\rho) < 0$ is satisfied by assumption, a feasible r^0 is found in a finite number of iterations in Step 1. Moreover, from $g(\chi,r^0) < 0$ it additionally follows that $r^0 \in \operatorname{int}(\Phi)$. Similarly, the update from r^k to r^{k+1} in Step 2 is achieved in a finite number of iterations. The number of evaluations needed in Step 1 and Step 2 depend on the stepsizes defined through $\alpha_1, \alpha_2 \in (0,1)$. However, since the optimization problem (46) has a strongly convex objective function, convergence $r^\kappa \to \rho^{\#_\ell}(\chi)$ in Algorithm 1 holds for $\kappa \to \infty$ independent of the selection of α_1 and α_2 [9, Section 9.5.3 and Section 11.3.3]. Nevertheless, a fixed number $\kappa \in \mathbb{N}$ is sufficient to update r^+ and to push it

Algorithm 1: Update of $r^+ = \omega(\chi, \rho, r)$

Input: Parameters $\ell > 0$, $\alpha_1, \alpha_2 \in (0,1)$, $\kappa \in \mathbb{N}$ and $\rho \in \operatorname{int}(\Phi)$, $r \in \Phi$, $\chi \in \operatorname{int}(\mathcal{E}_r(P))$.

Output: $r^+ = r^\kappa \in \operatorname{int}(\Phi)$.

1) **Step 1:** For $s \in \mathbb{N}$, compute $r^0 = \alpha_1^s r + (1-\alpha_1^s)\rho$ until $g(\chi, r^0) < 0$ is satisfied.
2) **Step 2:** For $k = 0, \dots, \kappa - 1$, compute

$$r_\Delta = -\left[\ell \nabla_\delta^2 h_0(r^k;\chi) + \nabla_\delta^2 \phi(r^k;\chi)\right]^{-1} \cdot \left[\ell \nabla_\delta h_0(r^k;\chi) + \nabla_\delta \phi(r_j;\chi)\right]$$

and for $s \in \mathbb{N}$ compute $r^{k+1} = r^k + (\alpha_2)^s r_\Delta$ until $g(\chi, r^{k+1}) < 0$ is satisfied.

towards the origin. In the limit, if $g(\chi, r^{\#_\ell}) = 0$ is satisfied, the update of ρ through π_ε ensures that $g(x, \rho^+) < 0$, i.e., $\rho^+ \in \operatorname{int}(\Phi)$ is strictly feasible when Algorithm 1 is initialized at the next discrete time step.

Lemma 5: Let $\alpha_1, \alpha_2 \in (0,1)$, let $\kappa \in \mathbb{N}$, assume Φ is bounded and define $M = \max_{\delta \in \Phi} |\delta|$. Moreover, for $\chi \in \operatorname{int}(\mathcal{R})$ define $\ell \in \mathbb{R}_{>0}$ such that

$$\ell \geq \frac{2\|A^\perp\|_2 d}{\sqrt{\lambda_{\min}(P)} M \beta(\rho^\star(\chi))}. \tag{48}$$

Then, the update $\rho^+ = \omega(\chi, \rho, r)$ defined through Algorithm 1 satisfies Property 1. ⌟

While (48) is not accessible since $\rho^\star(\chi)$ is not known under the assumptions in this section, the current reference point ρ, and in particular $\beta(\rho)$, can be used as an estimate for $\beta(\rho^\star(\chi))$. Moreover, while the statement of the lemma is restricted to the case that the set Φ is bounded, since $|\rho|$ is monotonically decreasing, M can be defined based on the initial condition $\rho_0 \in \Phi$.

Proof: Condition (44) together with the triangular inequality, the upper bound in (47) and the condition on ℓ in (47) ensure that the following chain of inequalities is satisfied:

$$\begin{aligned}(|\rho^{\#_\ell}| - |\rho^\star(\chi)|)(|\rho^{\#_\ell} - \rho^\star(\chi)|) &\leq (|\rho^{\#_\ell}| - |\rho^\star(\chi)|)(|\rho^{\#_\ell}| + |\rho^\star(\chi)|) \\ &= |\rho^\star|^2 - |\rho^{\#_\ell}(\chi)|^2 \leq \frac{d}{\ell} \\ &\leq \tfrac{1}{2\|A^\perp\|_2}\sqrt{\lambda_{\min}(P)} M \beta(\rho^\star(\chi)).\end{aligned}$$

Additionally, since $0 \leq |\rho^{\#_\ell}(\chi)| - |\rho^\star(\chi)| < M$ according to (47) and the definition of M, it further holds that

$$|\rho^{\#_\ell} - \rho^\star(\chi)| \leq \tfrac{1}{2\|A^\perp\|_2}\sqrt{\lambda_{\min}(P)}\beta(\rho^\star(\chi))$$

which completes the proof. ■

Algorithm 1 is one possible way to define function ω in the hybrid dynamics (42). However, while the function ω implicitly defined through Algorithm 1 satisfies Property 1 for appropriately selected parameters, ω is not outer semi-continuous due to the computation of r^k, $k \in \mathbb{N}$, depending on the calculation of a feasible stepsize. To guarantee outer semi-continuity, Step 1 in Algorithm 1 can be replaced by an update similar to the convex combination in (25) and the stepsize selection in Step 2 can be replaced by a sufficiently small constant stepsize. Here, a sufficiently small stepsize can be explicitly calculated based on the strong convexity of the objective function of (46) (see [9, Section 9.5.3], for example). Instead of going into these details, we illustrate the main results of this paper based on numerical examples in the next section.

VI. Numerical Illustration

We discuss two examples illustrating the size of the estimated region of attraction (ERA) and clarifying the nature of the closed-loop trajectories induced by our controllers.

Example 1: Consider the dynamics (3) defined through the matrices

$$A = \begin{bmatrix} 0.6 & -0.8 \\ 0.8 & 0.6 \end{bmatrix}, \qquad B = \begin{bmatrix} 1.2045 & 1.4183 \\ 0.1259 & 1.3739 \end{bmatrix} \tag{49}$$

together with the saturation limits

$$u^- = \frac{2}{3}\begin{bmatrix} 2 \\ 1 \end{bmatrix} \quad \text{and} \quad u^+ = \frac{2}{3}\begin{bmatrix} 1 \\ 2 \end{bmatrix}.$$

The dynamical system is taken from [22], [24, Chapter 9.4], where different Lyapunov functions and corresponding feedback laws stabilizing the origin are discussed. Here, we have scaled u^-, u^+ and the columns of B to satisfy Assumption 1. Estimates of the region of attraction using an asymmetric Lyapunov function (ALF) and a generalized ALF discussed in [22] and [24, Chapter 9.4], respectively, are shown in Figure 3 (left).

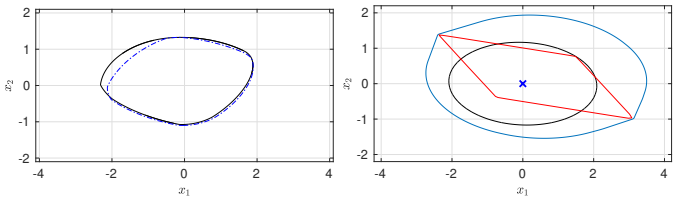

Fig. 3. Left: Estimates of the region of attraction given in [24, Chapter 9.4] and [22] through an asymmetric Lyapunov function (ALF) (blue — · —) and through a generalized ALF (black —). Right: Visualization of the ERA $\boldsymbol{\mathcal{E}_0(P)}$ (in black) together with $\boldsymbol{\mathcal{R}}$ (blue) for which convergence to the origin of the closed-loop system (34) and (42) are guaranteed through Theorems 1 and 2. Additionally the set of induced equilibria $\boldsymbol{x_e(\rho)}$, $\boldsymbol{\rho \in \Phi}$. is shown in red.

On the right, Figure 3 shows in blue the set $\mathcal{R}$, which is an estimate of the region of attraction of the origin for the closed-loop systems (34) and (42), according to Theorems 1 and 2. Additionally, the ERA $\mathcal{E}_0(P)$ obtained through Proposition 1 is visualized in black together with the set of induced equilibria $x_e(\rho)$ that can be stabilized through the saturated input $u \in [-u^-, u^+]$, shown in red. For Proposition 1 the parameter α is set to $\alpha = 0.05$, the parameters of the LMI in Proposition 1 are lower and upper bounded by -10 and 10, respectively, and X is set to zero, i.e., the gain L is not present in the corresponding controller.[2]

[2]Note that not only the ERAs of the origin in Figure 3 differ, but also the regions of attraction are different since different control laws are used to stabilize the origin.

We continue with an analysis of the closed-loop solution of the hybrid system (34) and (42), respectively, starting at $x_0 = \chi_0 = [-2.35, 1.35]^\top$. The remaining states of ξ_0 are initialized at zero. Figure 4 shows the closed-loop solution of (34) for different selections of $\underline{\tau}$, i.e., $\underline{\tau} \in \{0.001, 0.1\}$ and $\overline{\tau} = 0.1$. Since the system is initialized with $\rho = 0$, first

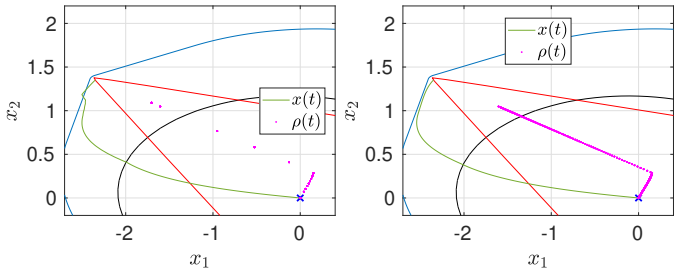

Fig. 4. Closed-loop solution of the hybrid system (34) for $\overline{\tau} = 0.1$ and different $\underline{\tau}$ (left: $\underline{\tau} = 0.1$; right: $\underline{\tau} = 0.001$).

a feasible $\rho \in \Phi$ needs to be determined (see Remark 9). Due to this fact, we observe that, in the case $\underline{\tau} = 0.1$, the set with guaranteed stability $\mathcal{R}$ (see Theorem 1) is left at the beginning of the simulation. As expected, once a feasible pair $(x, \rho) \in \mathcal{E}_\rho(P) \times \text{int}(\Phi)$ is found, the closed-loop solution $x(t)$ converges to zero as $t \to \infty$.

Figure 5 shows the closed-loop solution of (42). Here, in addition to the previous selections we fixed $\alpha_1 = \alpha_2 = 0.5$, $\ell = 100$ and $\kappa = 1$ (left) and $\kappa = 10$ (right) in Algorithm 1. For the function π_ε in Remark 7, the parameter $\varepsilon = 0.01$ is

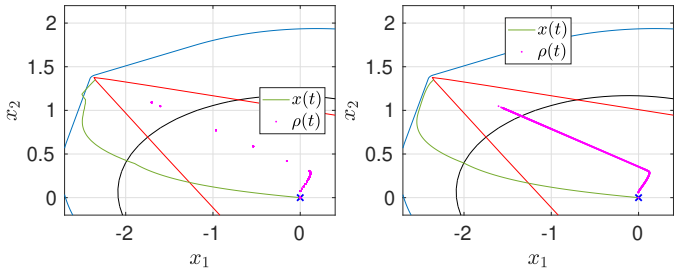

Fig. 5. Closed-loop solution of the hybrid system (42) for $\underline{\tau} = 0.1$, $\overline{\tau} = 0.1$ and $\kappa = 1$ on the left and $\underline{\tau} = 0.001$, $\overline{\tau} = 0.1$ and $\kappa = 10$ on the right. Additionally the parameter $\ell = 100$ is used for both settings.

used.

The time to evaluate the individual components of the controller dynamics in (34) and (42), corresponding to Figures 4 and 5 are shown in Figure 6 and Figure 7, respectively.

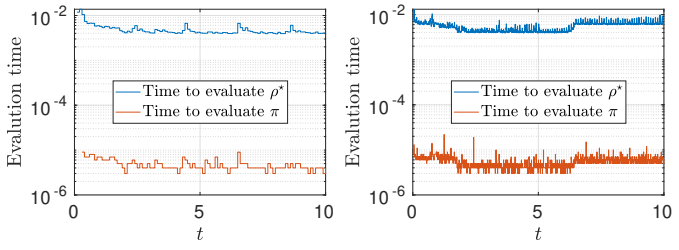

Fig. 6. Time to solve the optimization problem (19) and time to evaluate π between every discrete time update for the solutions in Figure 4.

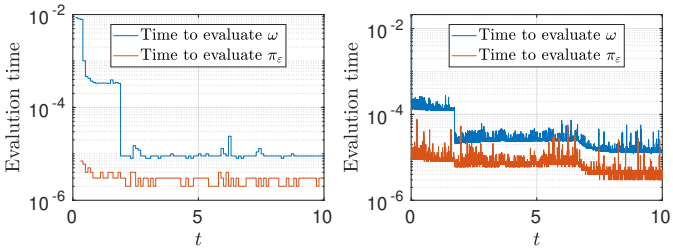

Fig. 7. Time to run Algorithm 1 and time to evaluate π_ε between every discrete time update for the solutions in Figure 5.

Based on these results, the time to evaluate π and π_ε does not seem to be restrictive. In particular, the inaccurate solution (42) of Section V, with the flexibility to select the number of iterations κ in Algorithm 1 small, allows for high sampling rates if necessary.

Example 2: We extend the two-dimensional dynamics discussed in Example 1 to the three dimensional system

$$A = \begin{bmatrix} 0.6 & -0.8 & 1.2045 \\ 0.8 & 0.6 & 0.1259 \\ 0 & 0 & 0 \end{bmatrix}, \quad B = \begin{bmatrix} 0 & 1.4183 \\ 0 & 1.3739 \\ 1 & 0 \end{bmatrix} \tag{50}$$

with the same saturation limits as in Example 1. The rationale of (50) is to perform a dynamic extension to represent rate saturation on the first input of the plant (49), as in [21]. Then, the magnitude saturated dynamics (50) comprises plant (49) with rate saturation on input 1 and magnitude saturation on input 2.

For this setting, the matrices $A^\perp$ and $B^\perp$ are given by

$$A^\perp = \begin{bmatrix} 0.3692 & -0.8019 \\ -0.5937 & -0.0784 \\ -0.7066 & -0.2720 \end{bmatrix}, \quad B^\perp = \begin{bmatrix} 0 & 0 \\ 0.1090 & 0.5261 \end{bmatrix}.$$

Since matrix A is not full rank, the two columns of $B^\perp$ are linearly dependent and the estimate of the region of attraction $\mathcal{R}$ guaranteed through Theorems 1 and 2 is unbounded. Figure 8 shows a chunk of $\mathcal{R}$ in a neighborhood around the origin in blue. Additionally, the sets $\mathcal{E}_0(P)$ and Φ are shown in red and black, respectively.

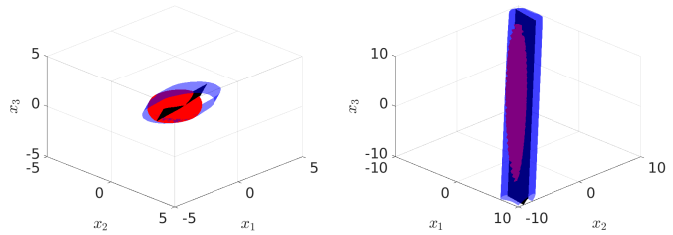

Fig. 8. Estimates of regions of attraction $\mathcal{R}$ (blue) and $\mathcal{E}_0(P)$ (red) from different angles for a three dimensional system. Additionally the set of stabilizable induced equilibria Φ is shown in black.

In Figure 9 and in Figure 10 the closed-loop solution and the evaluation times for the hybrid systems (34) and (42) are shown. Here, the system is initialized at $x_0 = \chi_0 = [-10, 13, 14]^\top$ and the same set of parameters as in the two-dimensional setting are used. Also in this case, the computation times shown in the figures illustrate the possible

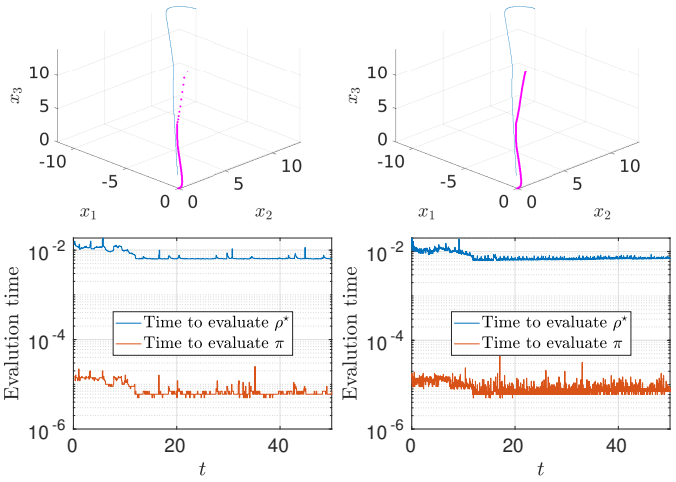

Fig. 9. Closed-loop solution and corresponding computation times of the hybrid system (34) for $\underline{\tau} = \mathbf{0.001}$, $\overline{\tau} = \mathbf{0.1}$ (left) and $\underline{\tau} = \overline{\tau} = \mathbf{0.1}$ (right).

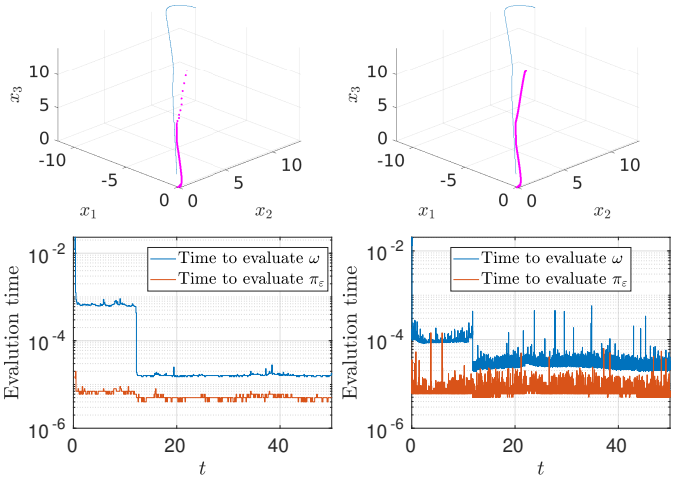

Fig. 10. Closed-loop solution and corresponding computation times of the hybrid system (42) for $\underline{\tau} = \mathbf{0.001}$, $\overline{\tau} = \mathbf{0.1}$ (left) and $\underline{\tau} = \overline{\tau} = \mathbf{0.1}$ (right). Additionally, κ in Algorithm 1 is defined as 1 (left) and 10 (right), respectively.

advantages stemming from the inaccurate solution discussed in Section V, which does not require the exact computation of $\rho^\star$. The numerical example shows that the proposed controller design is not restricted to the planar case and the controller can be equally applied in higher dimensions.

VII. Conclusions

In this paper we have derived a controller for linear systems with (asymmetric) input saturation that stabilizes the origin, with enlarged estimate of the region of attraction with convergence guarantees, by stabilizing a shifted equilibrium that is gradually driven to the origin in a sampled-data fashion.

To prove our main results, we have embedded the setting in a hybrid systems formalism, where the linear system evolves in continuous time, while the shifted equilibrium is updated at discrete times so that the intersample intervals can be used to solve nontrivial optimization problems. Our stability proofs require a deep investigation of the complex interplay between continuous-time dynamics and iterative parametric optimization schemes. The results are illustrated on numerical examples, showing advantages in terms of enlarged estimates for regions of attraction as compared to existing results.

References

[1] J.-P. Aubin. *Viability Theory*. Birkhäuser, 1991.

[2] J.-P. Aubin and A. Cellina. *Differential Inclusions: Set-Valued Maps and Viability Theory*. Springer, 1984.

[3] A. Bemporad, M. Morari, V. Dua, and E. N. Pistikopoulos. The explicit linear quadratic regulator for constrained systems. *Automatica*, 38(1):3–20, 2002.

[4] A. Benzaouia. Constrained stabilization: an enlargement technique of positively invariant sets. *IMA Journal of Mathematical Control and Information*, 22(1):109–118, 2005.

[5] A. Benzaouia, F. Mesquine, and M. Benhayoun. *Saturated Control of Linear Systems*. Springer, 2017.

[6] F. Blanchini, G. Giordano, F. Riz, and L. Zaccarian. Solving nonlinear deadzone-induced algebraic loops in bounded control of linear plants. *Submitted to the IEEE Transactions on Automatic Control*, 2021.

[7] F. Blanchini and S. Miani. Any domain of attraction for a linear constrained system is a tracking domain of attraction. *SIAM Journal on Control and Optimization*, 38(3):971–994, 2000.

[8] S. Boyd, L. El Ghaoui, E. Feron, and V. Balakrishnan. *Linear Matrix Inequalities in System and Control Theory*. SIAM, 1994.

[9] S. Boyd and L. Vandenberghe. *Convex Optimization*. Cambridge University Press, 2004.

[10] P. Braun, G. Giordano, C. M. Kellett, and L. Zaccarian. An asymmetric stabilizer based on scheduling shifted coordinates for single-input linear systems with asymmetric saturation. *IEEE Control System Letters*, 2021.

[11] A. L. Dontchev and R. T. Rockafellar. *Implicit Functions and Solution Mappings*. Springer, 2009.

[12] E. Garone and M. M. Nicotra. Explicit reference governor for constrained nonlinear systems. *IEEE Transactions on Automatic Control*, 61(5):1379–1384, 2016.

[13] E.G. Gilbert and I.V. Kolmanovsky. Set-point control of nonlinear systems with state and control constraints: a Lyapunov-function, reference-governor approach. In *Proc. of the 38th IEEE Conference on Decision and Control*, volume 3, pages 2507–2512, 1999.

[14] R. Goebel, R.G. Sanfelice, and A.R. Teel. *Hybrid Dynamical Systems: modeling, stability, and robustness*. Princeton University Press, 2012.

[15] A. Grancharova and T. A. Johansen. *Explicit Nonlinear Model Predictive Control: Theory and Applications*, volume 429. Springer Science & Business Media, 2012.

[16] M. Grant and S. Boyd. CVX: Matlab software for disciplined convex programming, version 2.1. http://cvxr.com/cvx, 2014.

[17] L. B. Groff, J. M. Gomes da Silva, and G. Valmorbida. Regional stability of discrete-time linear systems subject to asymmetric input saturation. In *Proc. of the 58th IEEE Conference on Decision and Control*, pages 169–174, 2019.

[18] L. Grüne and J. Pannek. *Nonlinear Model Predictive Control*. Springer International Publishing, 2017.

[19] T. Hu and Z. Lin. *Control Systems with Actuator Saturation: Analysis and Design*. Springer Science & Business Media, 2001.

[20] T. Hu, A. N. Pitsillides, and Z. Lin. Null controllability and stabilization of linear systems subject to asymmetric actuator saturation. In *Proc. of the 39th IEEE Conference on Decision and Control*, volume 4, pages 3254–3259, 2000.

[21] V. Kapila and W. M. Haddad. Fixed-structure controller design for systems with actuator amplitude and rate non-linearities. *International Journal of Control*, 73(6):520–530, 2000.

[22] Y. Li and Z. Lin. On the estimation of the domain of attraction for linear systems with asymmetric actuator saturation via asymmetric Lyapunov functions. In *American Control Conference*, pages 1136–1141, 2016.

[23] Y. Li and Z. Lin. An asymmetric Lyapunov function for linear systems with asymmetric actuator saturation. *International Journal of Robust Nonlinear Control*, 21(4):1–17, 2017.

[24] Y. Li and Z. Lin. *Stability and performance of control systems with actuator saturation*. Springer, 2018.

[25] J. Löfberg. YALMIP: a toolbox for modeling and optimization in MATLAB. In *IEEE International Conference on Robotics and Automation*, pages 284–289. IEEE, 2004.

[26] S. Mariano, F. Blanchini, S. Formentin, and L. Zaccarian. Asymmetric state feedback for linear plants with asymmetric input saturation. *IEEE Control Systems Letters*, 4(3):608–613, 2020.

[27] M. M. Nicotra and E. Garone. The explicit reference governor: A general framework for the closed-form control of constrained nonlinear systems. *IEEE Control Systems Magazine*, 38(4):89–107, 2018.

[28] A. Papachristodoulou, J. Anderson, G. Valmorbida, S. Prajna, P. Seiler, P. A. Parrilo, M. M. Peet, and D. Jagt. *SOSTOOLS: Sum of squares optimization toolbox for MATLAB*, 2021. Available from `https://github.com/oxfordcontrol/SOSTOOLS`.

[29] J. B. Rawlings, D. Q. Mayne, and M. Diehl. *Model Predictive Control: Theory, Computation, and Design*, volume 2. Nob Hill Publishing, 2017.

[30] W. J. Rugh and J. S. Shamma. Research on gain scheduling. *Automatica*, 36(10):1401–1425, 2000.

[31] S. Tarbouriech, G. Garcia, J.M. Gomes da Silva Jr., and I. Queinnec. *Stability and stabilization of linear systems with saturating actuators*. Springer-Verlag London Ltd., 2011.

[32] C. Yuan and F. Wu. Switching control of linear systems subject to asymmetric actuator saturation. *International Journal of Control*, 88(1):204–215, 2015.